The Dissertation Committee for Jiwoon Lee Certifies that this is the approved version of the following dissertation:

MOLECULAR MECHANISMS OF CHOROID FISSURE CLOSURE AND VENTRAL RETINA FORMATION IN THE ZEBRAFISH EYE

Committee:

Jeffrey M. Gross, Supervisor

Seema Agarwala

Janice Fischer

Jennifer Morgan

John Wallingford

MOLECULAR MECHANISMS OF CHOROID FISSURE CLOSURE AND VENTRAL RETINA FORMATION IN THE ZEBRAFISH EYE

by

Jiwoon Lee, B.S., M.S.

Dissertation

Presented to the Faculty of the Graduate School of

The University of Texas at Austin

in Partial Fulfillment

of the Requirements

for the Degree of

Doctor of Philosophy

The University of Texas at Austin

December, 2010

Acknowledgements

I thank my Lord, God for being with me. He has allowed me to study in Austin, Texas and has given me a great advisor, Jeff Gross. I sincerely appreciate Jeff for his advice and encouragement. I not only learned scientific knowledge from him but also how to live a wonderful life. I thank my parents and my sister, Ji-Inn for their continuous prayer and support. I thank all my committee members, Seema Agarwala, Janice Fischer, Jennifer Morgan, and John Wallingford for their time and warm advice. I thank Christina and all members of Gross lab for critical reading of this dissertation, and I also appreciate them because I was able to enjoy a wonderful time with them during the whole course of my Ph. D.

MOLECULAR MECHANISMS OF CHOROID FISSURE CLOSURE AND VENTRAL RETINA FORMATION IN THE ZEBRAFISH EYE

Publication No._____

Jiwoon Lee, Ph.D.

The University of Texas at Austin, 2010

Supervisor: Jeffrey M. Gross

During optic cup morphogenesis, the neuroectodermal layers of the optic vesicle (OV) invaginate ventrally, and fuse at the choroid fissure (CF) along the proximo-distal axis such that the retina and retinal pigment epithelium (RPE) are confined within the cup. Failure of CF closure results in colobomas, which are characterized by the persistence of a cleft or hole at the back of the eye. While CF closure is a critical aspect of ocular development, the molecular and cellular mechanisms underlying this process are poorly understood. My research examined CF closure and colobomas using zebrafish as a model system. In the first study, I determined that early cell fate changes within the eye field could cause colobomas using the zebrafish mutant *blowout*. Colobomas in *blowout* resulted from defects in optic stalk morphogenesis whereby the optic stalk extended into the retina and impeded the edges of the CF from meeting and fusing. Positional cloning of *blowout* identified a nonsense mutation in *patched1*, a negative regulator of the Hedgehog pathway. Up-regulation of Hedgehog pathway activity causes disruption in the patterning of the OV into proximal and distal territories, revealing that

cell fate determination, mediated by Hedgehog signaling, is intimately involved in regulating CF closure. In the second study, I examined Bcl6 function and regulation during zebrafish eye development. *bcl6* encodes a transcriptional repressor expressed in the ventral retina during zebrafish eye development. Loss of Bcl6 function leads to colobomas along with up-regulation of *p53*, a previously known Bcl6 target, and an increase in the number of apoptotic cells in the retina, demonstrating that Bcl6 plays a critical role in preventing apoptosis in the retina during early eye development. I also showed that Vax1 and Vax2 act upstream of *bcl6* in the ventral retina. Furthermore, I identified functional interactions between Bcl6, Bcor and Hdac1 during eye development, demonstrating that Bcl6 functions along with Bcor and Hdac1 to mediate cell survival by regulating *p53* expression. Together my studies expand the gene regulatory network involved in cell fate determination and cell survival during CF closure and ventral retina formation, and provide mechanistic insight into coloboma formation.

Table of Contents

List of Figures

CHAPTER I

INTRODUCTION – CHOROID FISSURE CLOSURE AND VENTRAL RETINA FORMATION

I. 1. VERTEBRATE EYE DEVELOPMENT

Vertebrate eye formation commences with the symmetric, bilateral evagination of optic vesicles (OV) from the diencephalon (Adler and Canto-Soler, 2007; Chow and Lang, 2001). Each OV then undergoes a complex series of morphogenetic movements that ultimately results in the formation of a bilayered optic cup, containing the prospective retina and retinal pigment epithelium (RPE). The optic cup remains attached to the diencephalon by the optic stalk, a transient structure that will eventually be filled by retinal ganglion cell axons and form the optic nerve. During optic cup morphogenesis, the neuroectodermal layers of the OV invaginate ventrally, and fuse along the proximo-distal axis such that the retina and RPE are confined within the cup (Fig I-1). Fusion occurs along a distinct ventral region of the optic cup called the choroid fissure. The choroid fissure is also a transient structure that allows for the exit of retinal axons into the optic nerve, and for the entrance of the hyaloid artery into the eye. These major events are well conserved between different vertebrates like human, mouse and zebrafish (Fig. I-2).

1

Evagination of optic primordia

↓

Formation of optic vesicle

↓

Invagination to form optic cup

↓

Fusion at choroid fissure

Choroid fissure

vOS NR RPE dOS
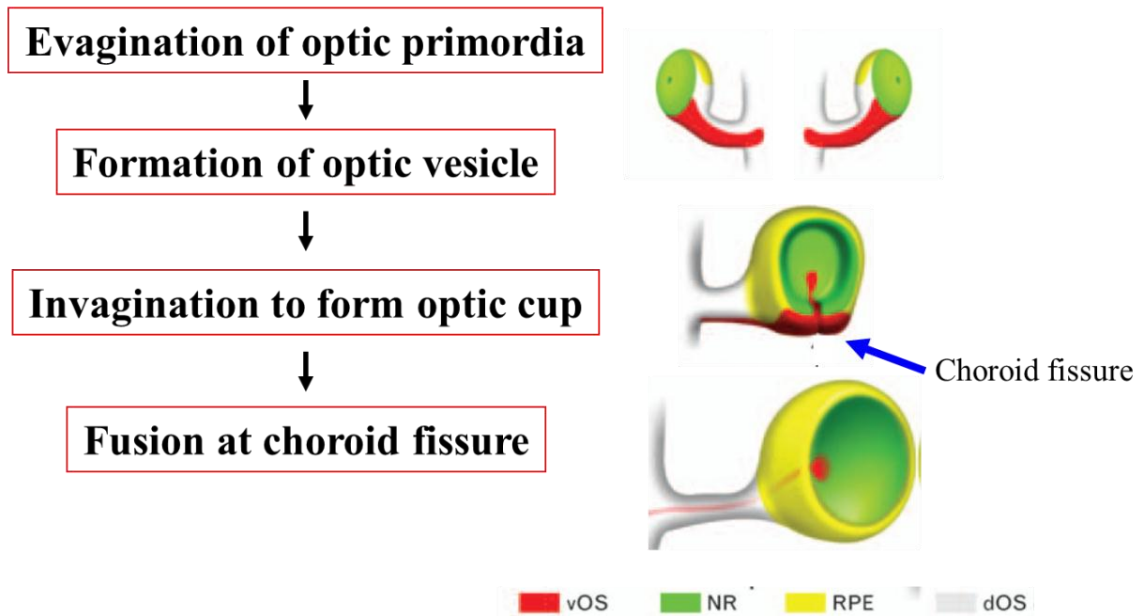
Modified from Chang et al., 2006

Figure I-1. The process of vertebrate eye development.

vOS, ventral optic stalk; NR, neural retina; RPE, retinal pigment epithelium; dOS, dorsal optic stalk.
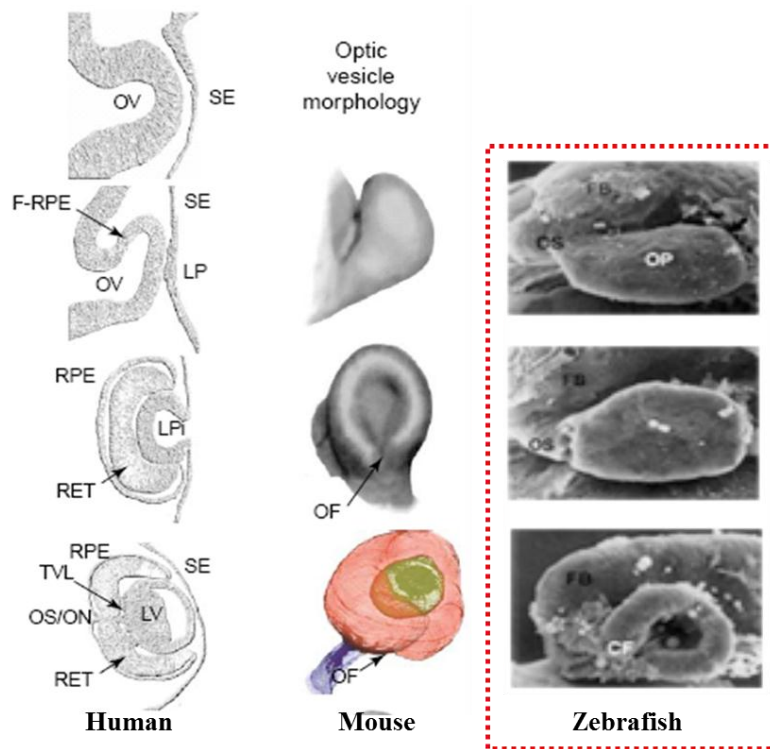
Modified from Fitzpatrick and van Heyningen, 2005.

Figure I-2. General aspects of eye development are well conserved between different vertebrates.

I. 2. COLOBOMAS

Defects in choroid fissure closure result in colobomas; ocular malformations characterized by the persistence of a cleft or hole at the back of the eye (Fig. I-3) (Chang et al., 2006; Fitzpatrick and van Heyningen, 2005; Gregory-Evans et al., 2004). Colobomas have a relatively high rate of incidence, ranging from 2.6 in 10,000 births in the U.S., to 0.75 in 10,000 births in China and are the cause of 3-10% of childhood blindness worldwide (Hornby et al., 2000; Porges, 1995). Colobomas are a phenotypic manifestation in over 50 distinct human genetic disorders (OMIM:http://www.ncbi.nlm.nih.gov/) and are often associated with other congenital abnormalities in the eye, including microphthalmia and anophthalmia (Bermejo and Martinez-Frias, 1998), as well as those of other organ systems. Multiple subtypes of colobomas have been described and depending on their severity colobomas can at a minimum lead to cosmetic defects and more commonly, they lead to complete blindness. The most severe types of these are chorioretinal colobomas in which large regions of the eye lack both retina and RPE tissue because the cells that would have given rise to them were not enclosed within the developing optic cup. While choroid fissure closure is a critical aspect of ocular development that requires a precise interplay between growth, morphogenesis and regulated gene expression, the molecular and cellular mechanisms underlying this process have not yet been fully elucidated in any vertebrate organism.

Normal Eye

Iris, Retina, Macula, Optic Nerve Coloboma
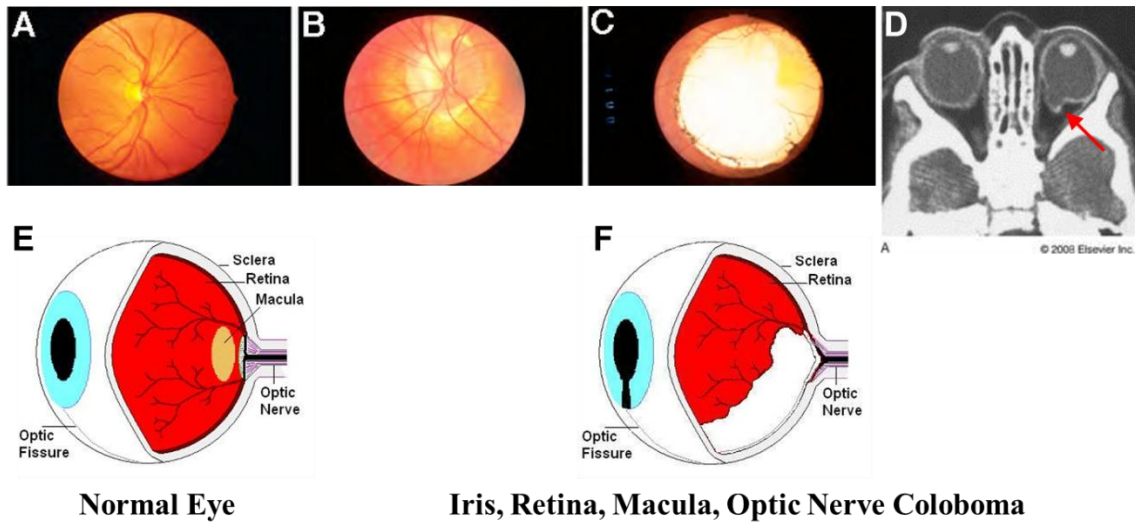
Figure I-3. Coloboma

(A,B,C) Human eye pictures taken from the back of the eye. (E,F) Cartoon of human eye. (A,E) Normal eye with well contained retina tissue with eye cup. (B,C,F) Large holes in the back of the eye and lack of the large part of the retina tissue. (D) CT image from coloboma patient shows extrusion of retina tissue (red arrow).

I. 3. HEDGEHOG SIGNALING PATHWAY DURING EYE DEVELOPMENT

Many developmental events in the OV are regulated by secreted signaling molecules of the Bone Morphogenetic Protein (BMP), Transforming Growth Factor Beta (TGF-β), Wnt, Fibroblast Growth Factor (FGF) and Hedgehog (Hh) families (Adler and Canto-Soler, 2007; Chow and Lang, 2001; Esteve and Bovolenta, 2006). Perhaps the best studied of these in early eye development is Hh, whose members regulate several aspects of OV formation, patterning and morphogenesis (Amato et al., 2004). Sonic hedgehog (Shh), secreted from the ventral midline, first functions in directing the separation of the eye field into two bilateral OVs in both mice and human embryos (Chiang et al., 1996; Roessler et al., 1996). In the zebrafish embryo, mutations in *Shh* do not lead to cyclopia likely due to redundancy with other Hh related proteins (Barresi et al., 2000; Karlstrom et al., 1999; Schauerte et al., 1998). A second key role for Shh signaling in the OV is to promote proximal cell fates (i.e. optic stalk and choroid fissure), and to repress distal cell fates (i.e. retina, RPE and lens) (Fig. I-4). The *pax2* transcription factor is a critical Shh target in this process; *pax2* expression in the optic stalk and choroid fissure is dependent on Shh (Chiang et al., 1996; Perron et al., 2003; Zhang and Yang, 2001) and *Shh* overexpression is sufficient to induce the expression of *pax2* in more distal OV territories where it is normally absent (Ekker et al., 1995; Macdonald et al., 1995; Perron et al., 2003; Zhang and Yang, 2001). *pax2* and *pax6* repress each other's transcription and thereby form a precise boundary between the optic stalk and retina (Schwarz et al., 2000). Loss of *pax2* function leads to optic nerve hypoplasia and colobomas in human patients,

dorsal

distal

Optic stalk   Wild-type   Shh

● *Pax2*
● *Pax6*

Inhibition of Shh signaling

Activation of Shh signaling
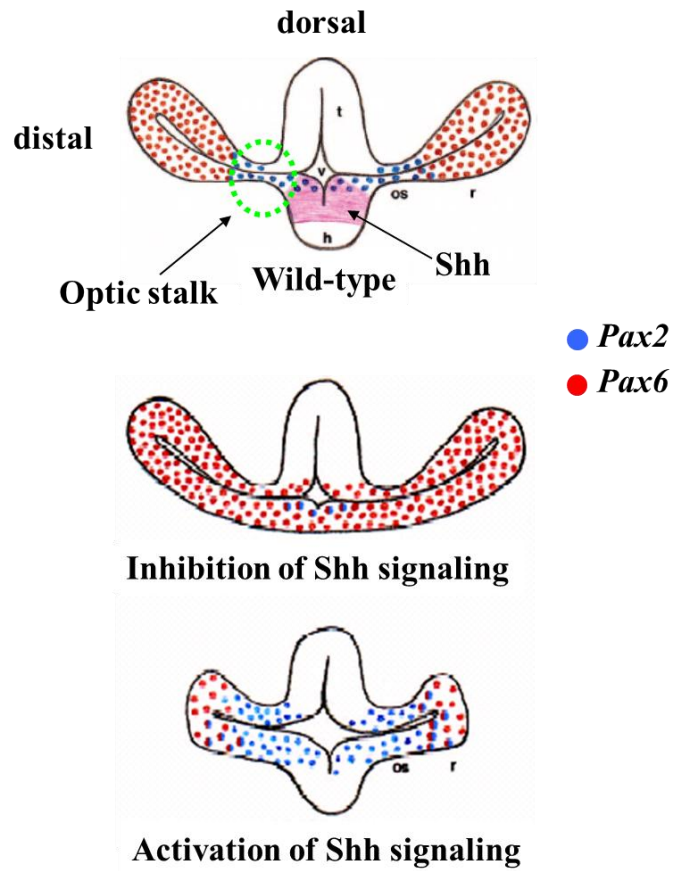
Modified from Macdonald et al., 1995

Figure I-4. Overview of cell fate changes in the OV depending on Shh signaling

as well as in a number of animal model systems, indicating that Shh signaling is critical for choroid fissure closure (Macdonald et al., 1997; Otteson et al., 1998; Sanyanusin et al., 1995; Schwarz et al., 2000; Torres et al., 1996).

I. 4. VAX1 AND VAX2 IN THE EYE FORMATION

Zebrafish provide an excellent model system in which eye development can be studied and through which the molecular mechanisms underlying human ocular diseases can be elucidated (Goldsmith and Harris, 2003; Gross and Perkins, 2008). Indeed, loss of function phenotypes for *aussicht, pax2a, vax1/vax2, fgf19, n-cadherin, apc, laminin β1* and *laminin γ1* each lead to colobomas in zebrafish and have been informative in furthering our understanding of choroid fissure closure *in vivo* (Gross and Perkins, 2008; Heisenberg et al., 1999; Nakayama et al., 2008). Of particular relevance in this group are the *vax1* and *vax2* genes. The *vax* genes are co-expressed in the optic stalk and ventral optic cup, with *vax1* enriched in the optic stalk and *vax2* enriched in the ventral optic cup (Barbieri et al., 1999; Hallonet et al., 1998; Ohsaki et al., 1999; Take-uchi et al., 2003). Similar to *pax2*, at these early developmental stages *vax1/vax2* gene expression is also dependent on *Shh* (Perron et al., 2003; Take-uchi et al., 2003), and *Shh* overexpression is sufficient to increase both *vax1* and *vax2* levels (Sasagawa et al., 2002; Zhang and Yang, 2001). Targeted knockout of either *vax1* or *vax2* leads to ventral optic cup defects and colobomas in mouse (Barbieri et al., 2002; Bertuzzi et al., 1999; Hallonet et al., 1999; Mui et al., 2002), and similarly, morpholino disruption of *vax1* and *vax2* results in ventral optic cup defects and colobomas in zebrafish (Take-uchi et al., 2003). The *vax* proteins

8

function in the optic stalk and ventral optic cup by repressing *pax6* expression to promote proximal OV fates over more distal ones (Mui et al., 2005; Take-uchi et al., 2003). Combined, what emerges from these studies is a model in which *Shh* signaling activates *pax2* and *vax1/vax2* dependent pathways, where the *pax2* pathway directly regulates optic stalk and choroid fissure formation while the *vax1/vax2* pathway represses retina and RPE differentiation in the optic stalk and ventral optic cup.

Although defects in choroid fissure closure result in colobomas and incidences of colobomas are relatively high within the human population, the molecular mechanisms and the cellular processes that facilitate choroid fissure closure have not been well characterized in any vertebrate organism. The molecular basis of the defects underlying colobomas is largely unknown and there are few experimentally tractable animal models for studying their etiology. Here, my studies utilized the zebrafish, *Danio rerio,* to elucidate the mechanisms that underlie ventral retina formation and choroid fissure closure. Many disrupted genes and pathways identified as integral to the formation of the zebrafish eye produce phenotypes that resemble disorders of the human visual system (Gross and Perkins, 2008; Goldsmith and Harris, 2003). Thus, characterization of the molecular mechanisms of eye development in zebrafish will shed light on the molecular and morphogenetic defects that lead to colobomas in humans.

CHAPTER II

Zebrafish *blowout* provides genetic evidence for *patched1*-mediated negative regulation of hedgehog signaling within the proximal optic vesicle of the vertebrate eye

II. 1. BACKGROUND

With an interest in better understanding the molecular mechanisms underlying OV morphogenesis and choroid fissure closure, I have positionally cloned and characterized a recessive zebrafish mutant named *blowout* (*blw*), that was originally identified in the large-scale mutagenesis screen in Tübingen (Karlstrom et al., 1996). *blw* mutants possess colobomas and defects in retinotectal projections, although visual function is relatively normal when tested in optokinetic response assays and by electroretinograms (Karlstrom et al., 1996; Neuhauss et al., 1999). Positional cloning of *blw* revealed a nonsense mutation in *patched1* (*ptc1*) as the cause of these ocular defects. Loss of *ptc1* function leads to an expansion of Hh target gene expression in *blw* mutants. Within the OV, *pax2a* expression is expanded distally at the expense of *pax6* and as a result, the optic stalk expands into the ventral optic cup. This appears to physically prevent the lateral edges of the choroid fissure from meeting and fusing. Blocking Hh pathway activity with cyclopamine suppressed colobomas in *blw* mutants, indicating that constitutive Hh pathway activity is likely the molecular mechanism underlying the coloboma phenotype in *blw*. These observations highlight the critical role that Hedgehog

10

pathway activity plays in mediating patterning of the proximal/distal axis of the optic vesicle during the early phases of eye development, and they provide genetic confirmation for the integral role that *patched1*-mediated negative regulation of Hedgehog signaling plays during vertebrate eye development.

II. 2. RESULTS

II. 2. 1. *Blowout* mutants possess defects in choroid fissure closure

blw mutants present with obvious colobomas (Fig. II-1A–D). In mutants, the choroid fissure has not closed and as a result, retinal and RPE tissue are not contained within the eyecup (Fig. II-1E–I). Severity of the phenotype varies between homozygous embryos with phenotypes ranging from subtle, unilateral colobomas in some embryos to severe, bilateral colobomas in others. Retinal and RPE tissue extend from the eyecup into the forebrain in the most severely affected mutants (Fig. II-1I), while in those less severely affected, a cleft is observed surrounding the choroid fissure but little to no retinal tissue has expelled through this cleft (Fig. II-1H). Penetrance of the phenotype also varies between clutches, ranging from 3% – 22% of total embryos in any given clutch derived from heterozygous parents developing a coloboma. Within the eye, beyond these containment defects, other aspects of development and patterning appear normal. Lens and RPE formation are unaffected, retinal lamination is normal and all retinal cell types are present in mutant embryos (Figure II-2 and *data not shown*). Retinal ganglion cell axons are not bundled at the optic nerve and as a result, the nerve is often
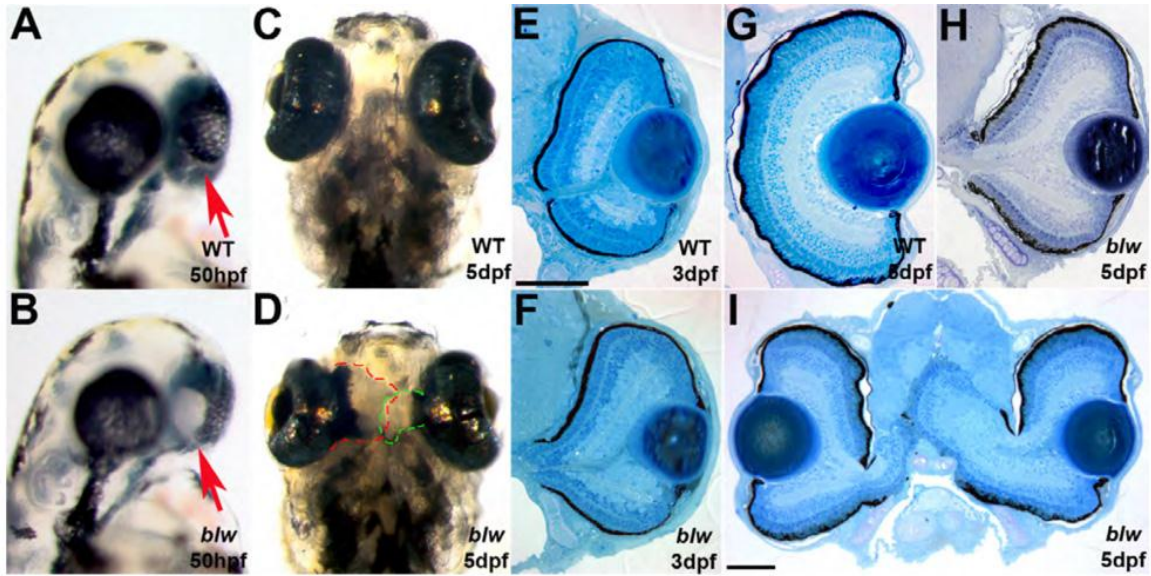
Figure II-1. *blowout* mutants present with colobomas.

Wild-type (A,C) and *blw* (B,D) mutant embryos at 50hpf (A,B) and 5dpf (C,D) imaged laterally (A,B) and ventrally (C,D). Colobomas can be unilateral or bilateral, and these *blw* mutants show bilateral incidence. Arrows in A,B point to the choroid fissure. Retinal tissue expelled from each eye has been outlined to illustrate the extent of the coloboma in C,D. Transverese histological sectioning of wild-type (E,G) and *blw* (F,H,I) eyes. Colobomas are obvious at 3dpf in *blw* (F); however, at later time points their severity varies ranging from mild (H) to severe (I). Lens and retinal development appear normal in *blw* mutants. Anterior is up in A–D. Dorsal is up in E–I. Scale bars are 100um.
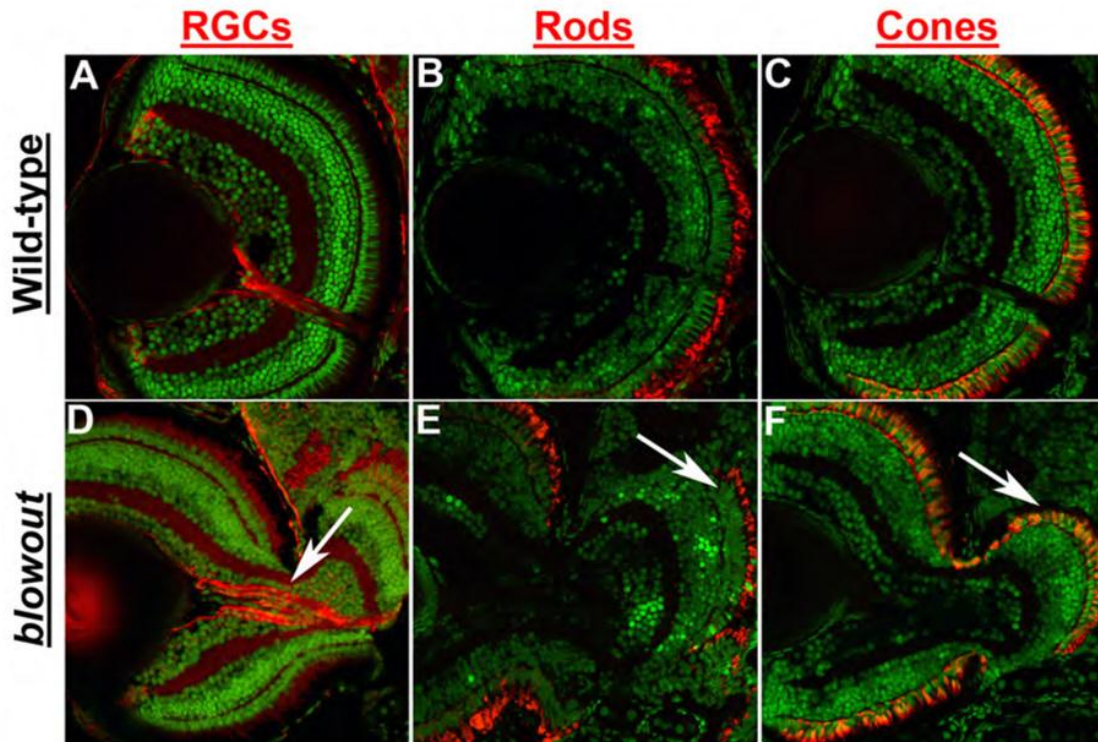
Figure II-2. Retinal development is largely normal in *blowout*.

Immunohistochemical analysis of retinal ganglion cells (RGCs) via zn8 staining (A,D), rod photoreceptors via zpr3 staining (B,E) and red/green double cones via zpr1 staining (C,F) in transverse retinal cryosections. All retinal cell types are present and are properly distributed in *blw* mutants, and retinal cell numbers are also similar between wild-type and *blw* mutant eyes. RGC organization is affected in *blw* mutants where RGC axons do not assemble into a tight bundle as they exit the eye (arrow in D). Photoreceptor outer segments are present in the retinal territories that are not contained within the eye cup (arrows in E,F). Antibody stains are red and nuclei are counterstained green with Sytox Green. Dorsal is up in all images.

split into two or more tracts that exit the eye through the colobomatous choroid fissure opening (Fig. II-2D). Indeed, retinotectal pathfinding defects have been previously described for this mutant and these may result from this inability to assemble the axons into a tight bundle as they exit the eye (Karlstrom et al., 1996). Interestingly, the region of the retina that extends from the eyecup and into the forebrain develops photoreceptors with fairly normal outer segment morphology as demonstrated by immunostaining for rhodopsin (Fig. II-2E) and red/green cone opsin (Fig. II-2F), indicating that apposition to the RPE is not necessary for outer segment morphogenesis.

II. 2. 2. Colobomas in *blowout* are not likely a result of retinal overproliferation or an absence of Bruch's membrane

Overproliferation within the retinal neuroepithelium has been shown to lead to colobomas (Kim et al., 2007) and thus, I first tested the hypothesis that retinal cells overproliferated in *blw* leading to a rupture of the optic cup, and an expulsion of retinal tissue into the forebrain. Proliferation was assessed using BrdU incorporation assays, and BrdU exposures were performed spanning several time points of development (e.g. 24–36hpf, 42–48hpf and 72–96hpf; Fig. II-3A,B and *data not shown*). BrdU incorporates into DNA during S-phase and serves as a useful readout of cell proliferation over a given time period. Quantification of the number of BrdU positive cells over these exposure periods revealed that they were present in similar numbers and location to those in wild-type siblings (Fig. II-3C and *data not shown*) indicating that that overproliferation of the retina is not likely to underlie the *blw* phenotype.

14
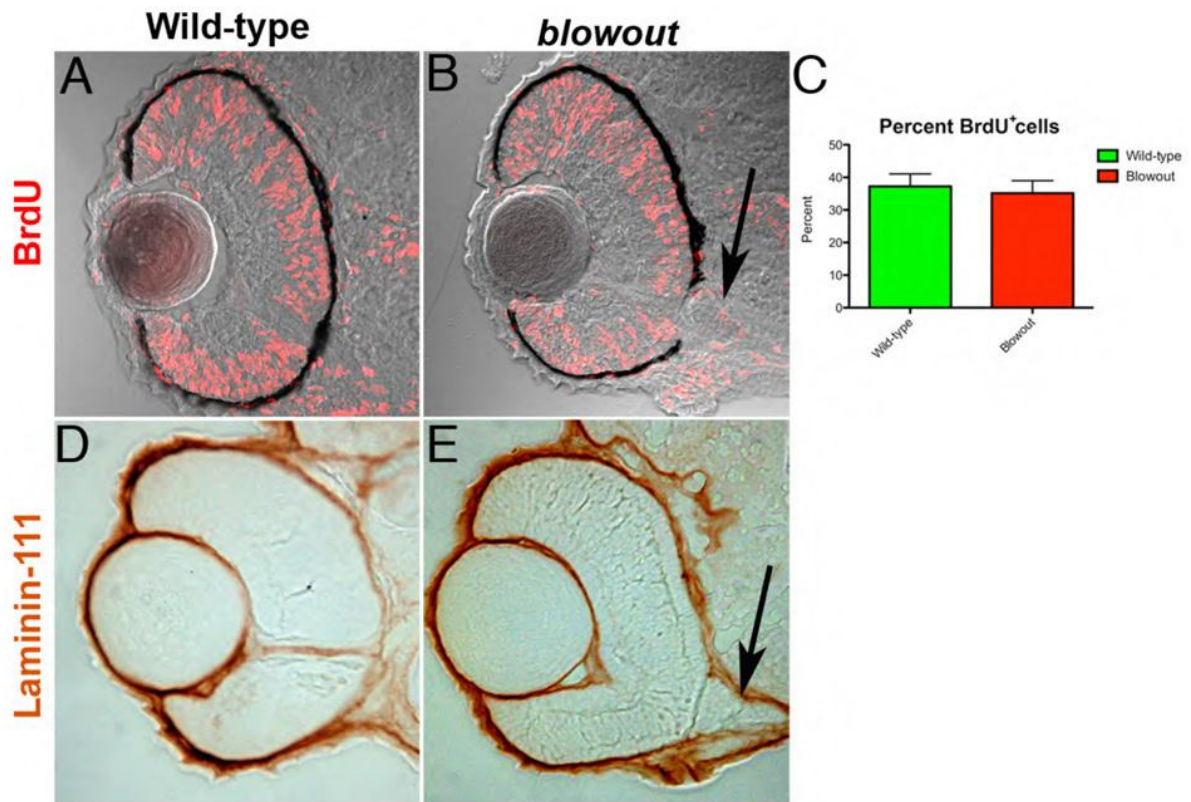
Figure II-3. Retinal cell proliferation and Bruch's membrane formation are both normal in *blowout*.

(A,B) Wild-type (A) and *blw* (B) embryos were exposed to BrdU from 42hpf to 48hpf and immediately sacrificed. BrdU positive cells (red) are observed throughout the retinas of wild-type and *blw* mutant embryos in similar proportions (C; no statistical difference - Fisher's exact test). Additional exposure periods (24–36hpf, 72–96hpf) resulted in identical regions of proliferation in the retinas of wild-type and *blw* mutants (*data not shown*). (D,E) Bruch's membrane, a basement membrane at the posterior of the eye, highly expresses the laminin-111 protein (Lee et al., 2007). Shown here are images of 12um cryosections from wild-type (D) and *blw* (E) whole-mount embryos stained for laminin-111 protein at 48hpf. Laminin-111 levels and distribution are similar between wild-type and *blw* embryos. The optic stalk appears abnormal in *blw*, as it remains connected to the retina at 48hpf (arrows in B,E), while in wild-type siblings it has degenerated. Transverse sections, dorsal is up in all images.

Basement membrane abnormalities are also known to contribute to colobomas (Gross et al., 2005; Hero et al., 1991; Lee and Gross, 2007), so I next tested the hypothesis that basement membrane defects might underlie the colobomas in *blw*. Bruch's membrane is a retinal basement membrane that separates the RPE from the choriocapillaris at the posterior of the eye and thus provides a physical barrier containing the retina and RPE within the optic cup. Laminin-111 protein is highly expressed in Bruch's membrane (Lee and Gross, 2007), so I utilized an antibody against laminin-111 to determine if Bruch's membrane was present in *blw* mutants. At all time points examined, laminin-111 levels in *blw* were comparable to those in wild-type embryos (Fig. II-3D,E). While this observation suggests that Bruch's membrane is unaffected in the mutants, laminin-111 is not expressed in the colobomatous area because the retina and RPE are expelled through this region. Therefore, while Bruch's membrane appears normal in *blw* mutants, I cannot rule out the possibility that there might be lower laminin-111 levels in the region of the choroid fissure and that these reduced levels compromise retinal containment and contribute to the colobomas in *blw*. Additional histological and molecular evidence described below makes this an unlikely scenario, however.

II. 2. 3. Optic stalk formation is abnormal in *blowout*

In examining DIC images from *blw* mutant retinal cryosections and laminin-111 expression in *blw*, I observed maintenance of the optic stalk in *blw* mutants relative to wild-type embryos in which the optic stalk had degenerated by this time (arrows in Fig.

II-3B,E). This prompted us to examine abnormalities in optic stalk formation as a potential cause of the colobomas in *blw*. When one closely examines embryos derived from *blw* heterozygous incrosses at very early stages of development (~20–24hpf), a thicker and expanded optic stalk is observed in a subset of these embryos, suggesting that optic stalk defects might underlie colobomas in *blw* mutants (*data not shown*). To directly analyze optic stalk formation in *blw* I performed serial histological sectioning on several mutants and their wild-type siblings at 31hpf (Fig. II-4). By examining serial sections taken at the same plane in both wild-type and *blw* mutants, the optic stalk appeared to be larger in the mutants than that in wild-type siblings (Fig. II-4B). Moreover, the optic stalk was kinked, and stalk tissue was ectopically located within the choroid fissure, appearing to physically prevent the fusion between its lateral edges (arrow in Fig. II-4B).

I wanted to further examine the optic stalk phenotype in *blw* to determine if optic stalk defects also manifest molecularly with an expansion of the proximal OV marker *pax2a* and a contraction of the distal OV marker *pax6*, which would suggest shifts in cell fate boundaries within the OV from retina to optic stalk. *pax2a* expression is normally limited to the region of the OV fated to become optic stalk as early as 15hpf (Fig. II-5A) and by 18hpf, as the OV has fully evaginated from the diencephalon, *pax2a* expression clearly demarcates the optic stalk territory of the OV from the remainder of the OV (Fig. II-5B). In *blw* mutants, the *pax2a* expression domain has expanded more distally into the remainder of the OV (Fig. II-5D,E) suggesting that proximal OV fates are expanded at the expense of distal ones. Indeed, the *pax6* expression domain is contracted in *blw* mutants in a pattern complementary to the expansion of *pax2a* (Fig. II-5C,F). This

17
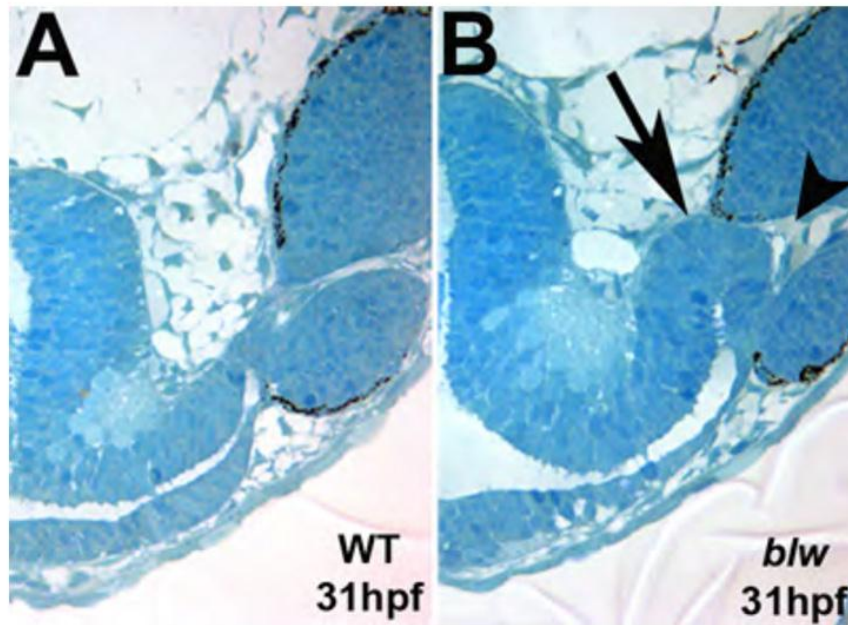
Figure II-4. Optic stalk morphology is abnormal in *blowout*.

Single 1.25um oblique histological sections taken from 31hpf wild-type (A) and *blw* (B) embryos taken at the same plane of sectioning. The optic stalk in *blw* is larger and kinked at the distal end (arrow in B). Optic stalk tissue is present at the choroid fissure and appears to prevent the lateral edges of the fissure from meeting and fusing (arrowhead).
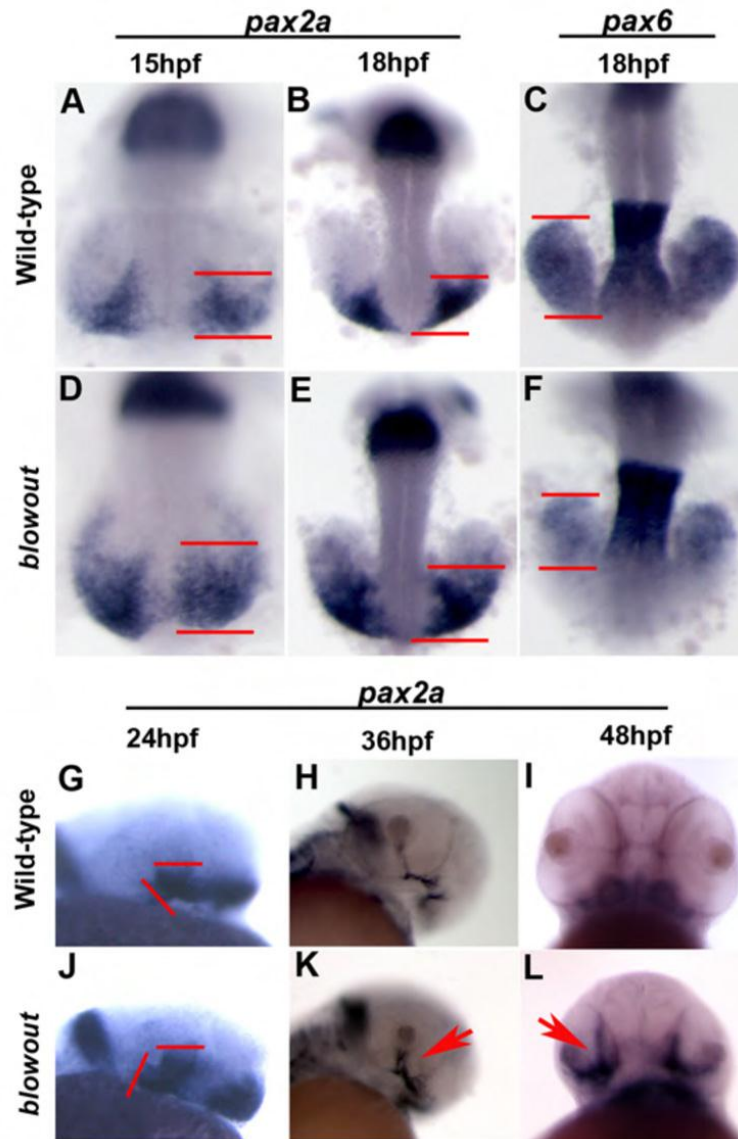
Figure II-5. The proximal/distal axis of the optic vesicle is disrupted in *blowout*.

pax2a marks the proximal OV (optic stalk) in wild-type embryos at 15hpf (A), 18hpf (B), 24hpf (G) and 36hpf (H), while it is absent at 48hpf (I) owing to the degeneration of the stalk by this time. Expression in *blw* mutants is observed in a broader domain within the optic stalk region as early as 15hpf (B) and this expansion is maintained at 18hpf (E), 24hpf (J) and 36hpf (K, arrow). Expression is not extinguished at 48hpf and can be observed to extend into the retina (L, arrow). Conversely, *pax6* marks the distal optic vesicle (retina and RPE) at 18hpf (C), and expression is substantially contracted within distal optic vesicle of *blw* mutants (F) in a pattern complementary to the expanded domain of *pax2a*.

19

observation strongly suggests that proximal/distal patterning of the OV is disrupted in *blw* mutants during the early phases of eye development.

pax2a also serves as a useful marker of the optic stalk at 24hpf (Fig. II-5G) and 36hpf (Fig. II-5H). In *blw* mutants, the *pax2a* expression domain has substantially expanded and now extends into the retina (Fig. II-5J,K). Moreover, while *pax2a* expression is nearly absent from the wild-type eye at 48hpf, concomitant with optic stalk differentiation (Fig. II-5I), in *blw* mutants expression is not only maintained but it also appears to spread into the retina (Fig. II-5L). Interestingly, in some embryos I noted asymmetric changes in *pax2a* expression where one optic stalk would show a large increase and the other would show either a more moderate increase or no change from wild-type levels (*data not shown*). As stated above, in some *blw* mutants, colobomas are unilateral while in others they are bilateral and thus, it appears that this asymmetry manifests at the molecular level as well as the morphological.

II. 2. 4. Positional cloning of *blowout*

To enable a molecular characterization of *blw* and its optic stalk phenotypes, I next set out to positionally clone the gene and identify the responsible mutation. Linkage mapping with microsatellite markers placed the mutation on chromosome 2, between Z11410 and Z13521. High-resolution mapping was then performed using additional microsatellite markers to refine the *blw* locus. Using markers z8451 and CH211-261P7-SSR2, and 526 *blw* mutant embryos, I defined a critical interval that must contain the
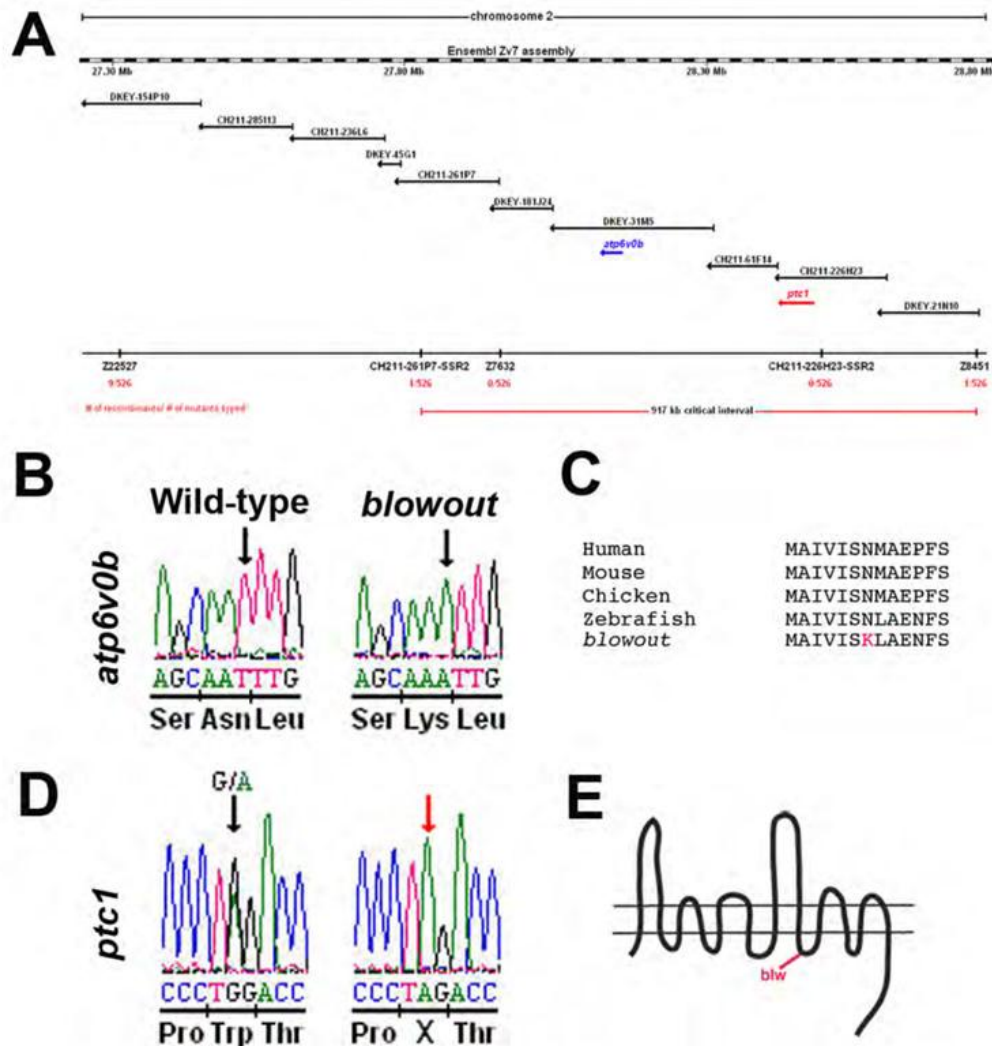
Figure II-6. Positional cloning of the *blowout* mutation.

(A) Genetic map of Chromosome 2 containing the *blw* mutation. Microsatellite markers and BACs are indicated with the number of recombinants and embryos genotyped. (B) Sequence chromatogram showing the *atp6v0b* mutation in *blw*. DNA sequence from wild-type (left) and homozygous (right) *blw* mutants are shown and the affected base is marked by an arrow. Amino acid sequence is listed below the DNA sequence. (C). Asn113, changed to Lys in *blw* (red), is conserved in vertebrate atp6v0b proteins. (D) Sequence chromatogram showing the *ptc1* mutation in *blw*. DNA sequence from heterozygous (left) and homozygous (right) *blw* mutants are shown and the affected base is marked by an arrow. (E) Schematic of the patched1 protein and the approximate position of the stop codon in *blw* situated after the 8th transmembrane domain.

21

blw locus (Fig. II-6A). Assembly of BACs spanning this region identified ten genes and one pseudogene within it (Fig. II-6A and *data not shown*). cDNAs representing six of these genes were cloned and sequenced and, interestingly, separate mutations in two different genes were identified in all 526 *blw* mutant embryos.

The first mutation identified was a missense mutation in *atp6v0b* (NM_199561) that changed bp520 from T-to-A, resulting in a nonconservative Asn to Lys change at position 113 of the protein (Fig. II-6B; www.ensembl.org/Danio_rerio). *atp6v0b* encodes a 22kDa proteolipid subunit (v0c") of the vacuolar ATPase complex (v-ATPase). The v-ATPase is a multi-protein complex consisting of thirteen different subunit types that are assembled stoichiometrically into a multimeric protein complex (Nishi and Forgac, 2002). v-ATPases are best known for their roles in H$^+$ transport through which they are important for intracellular and extracellular acidification events, protein transport and membrane fusion (Nelson and Harvey, 1999; Nishi and Forgac, 2002). Additionally, several recent studies have identified v-ATPase complex-independent functions for individual v-ATPase subunits (Hiesinger et al., 2005; Kontani et al., 2005), and perhaps the most interesting of these is in *C. elegans* where v0 subunits have been shown to be involved in mediating the release of Hedgehog-like ligands (Liegeois et al., 2006). The v0c" protein is highly conserved in eukaryotes and prokaryotes and Asn113 is also conserved in vertebrate v0c" proteins, suggesting that it may be important for protein function (Fig. II-6C). The second mutation I identified in *blw* was a nonsense mutation in *patched1* (*ptc1*; NM_130988) that changes bp3119 from G-to-A, resulting in a premature stop codon at position 1040 of the Patched1 protein (Fig. II-6D;

22

http://www.ncbi.nlm.nih.gov/entrez). This truncates Patched1 just after the 8th transmembrane helix (Fig. II-6E). Patched1 is a receptor for Hh ligands and in the unoccupied state, it serves as a negative regulator of Hh signaling by inhibiting the Smoothened protein. Upon binding of a Hh ligand by Patched, inhibition of Smoothened is relieved and a Hh dependent intracellular signaling pathway begins. Two *patched* genes are found in zebrafish, *ptc1* and *ptc2* (Concordet et al., 1996; Lewis et al., 1999), and *ptc1* is strongly expressed in the optic stalk during the stages of OV morphogenesis (Lewis et al., 1999). Ocular defects have not been described in *ptc1* morphants (Beales et al., 2007; Wolff et al., 2003), and OV morphogenesis does not appear to be disrupted in the zebrafish *ptc2* mutant, *leprechaun* (Koudijs et al., 2005).

II. 2. 5. Loss of patched1 function is responsible for the *blowout* phenotype

ptc1 is expressed in the zebrafish optic stalk (Fig. II-9A,C) (Lewis et al., 1999), and gene expression therein is known to be dependent on Hh signaling (Macdonald et al., 1995; Take-uchi et al., 2003) making *ptc1* a likely candidate for underlying the *blowout* phenotype. Indeed, that I observe Hh overexpression-like phenotypes in *blw* (e.g. expansion of *pax2a* expression at the expense of *pax6* expression) supports the hypothesis that loss of *ptc1* function may underlie these phenotypes. To determine if loss of *ptc1* function leads to colobomas, I injected a translation blocking MO targeting the *ptc1* transcript into 1-cell embryos (after Wolff et al., 2003). Knock-down of *ptc1* translation resulted in severe colobomas in all injected embryos, as well as additional
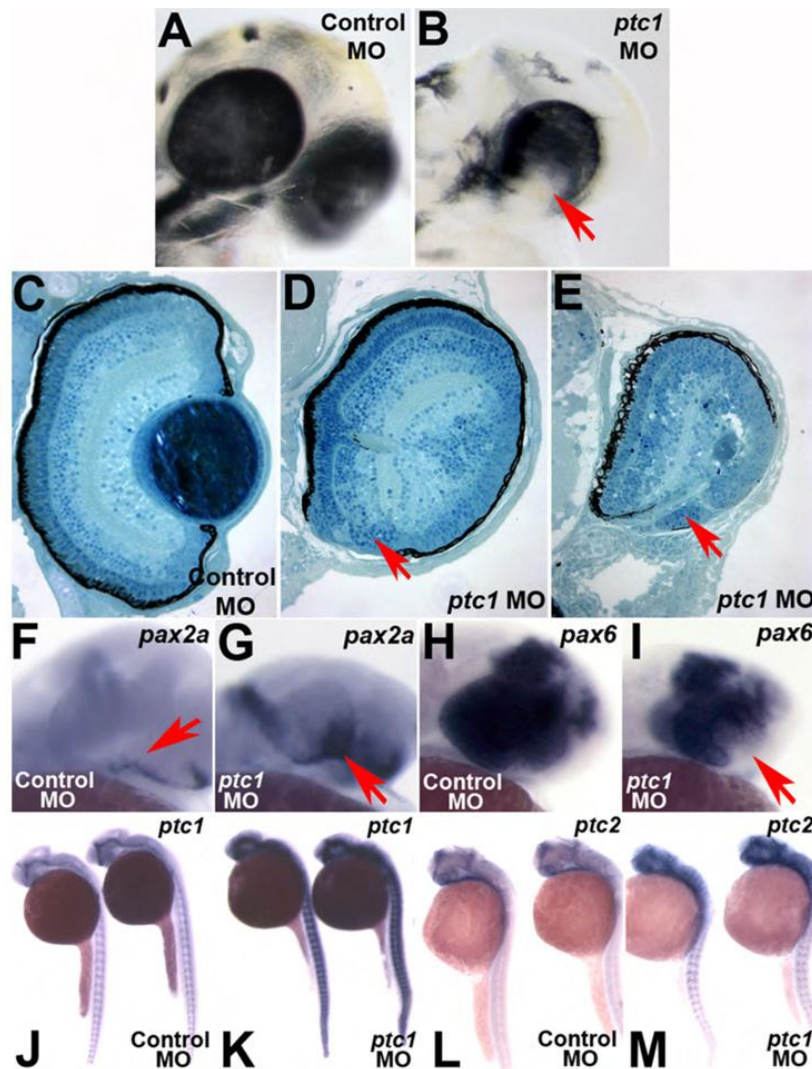
Figure II-7. Loss of *ptc1* leads to colobomas and ventral optic cup defects.

1.3ng injection of a translation blocking morpholino targeting *ptc1* transcripts (*ptc1*MO) results in colobomas. Lateral views of a (A) Control morpholino (ControlMO) injected and (B) *ptc1* morphant at 2.5dpf. Morphants possess bilateral colobomas (arrow in B). Morphants are more severely affected than *blw* mutants, showing medial displacement and lateral flexure of the eyes, and lens displacement. Overt brain and muscle defects are also observed. (C–E) Transverse histological sections from a 5dpf wild-type (C) and *ptc1* morphants (D,E). Severe colobomas are obvious in the morphants (arrows in D,E), and in the many of them the lens is also displaced and lies out of the plane of the section. *pax2a* expression is expanded into the retina at 24hpf (F,G) and *pax6* expression is contracted (H,I). The Hh target genes *ptc1* (J,K) and *ptc2* (L,M) also show expanded domains of expression in *ptc1* morphants.

24

overt phenotypes in the eye, brain and muscles (Fig. II-7A,B and *data not shown*). Histological analysis of *ptc1* morphants confirmed the degree to which the eye is affected in these embryos (Fig. II-7C–E). Colobomas in *ptc1* morphants were often more severe than those observed in *blw* and the eyes of *ptc1* morphants are rotated laterally relative to wild-type embryos, and their overall position is displaced medially, likely owing to the substantial coloboma and ventral retina defects. Many *ptc1* mutants also showed small, displaced lenses, a phenotype that does not appear in *blw* mutants. The lens phenotype in *ptc1* morphants is identical however to that reported to occur as a result of *Shh* overexpression where lens tissue is substantially reduced or absent (Barth and Wilson, 1995; Dutta et al., 2005; Yamamoto et al., 2004). Unfortunately, rescue experiments via injection of full-length *ptc1* mRNA into *blw* mutants and/or *ptc1* morphants were not successful, possibly owing to the large size of the *ptc1* transcript and/or degradation of the mRNA once injected (*data not shown*). Thus, the biological relevance of the increased severity of the *ptc1* morphant phenotype remains uncertain. However, and of particular note, molecular changes in *ptc1* morphants are identical to those observed in *blw* mutants where *pax2a* expression is expanded and extends into the retina (Fig. II-7F,G) and *pax6* expression is contracted (Fig. II-7H,I). These results support the hypothesis that loss of *ptc1* function is very likely to be the underlying cause of the colobomas in *blw*.

I also wanted to determine if *atp6v0b*[N113K] was causative or if it contributed to the colobomas observed in *blw*. As mentioned above, v0 subunits have been shown to be involved in mediating the release of Hedgehog-like ligands in *C. elegans* (Liegeois et al.,

2006). Changes in *pax2a* and *pax6* expression are hallmark molecular readouts of Hh overexpression phenotypes in the eye and that I observe such changes in *blw* (Fig. II-5) made it possible to envision a scenario whereby the $atp6v0b^{N113K}$ mutation could underlie or contribute to these ocular defects.

Five recessive mutations in different v-ATPase complex subunits have been identified in zebrafish, as well as a mutation in a v-ATPase associated protein (Amsterdam et al., 2004) and we have previously demonstrated that v-ATPase function is required for normal eye development (Gross et al., 2005). These v-ATPase roles, however are largely in regulating RPE pigmentation, in mediating RPE/photoreceptor interactions and in regulating cell survival in the ciliary marginal zones of the retina (Nuckels et al., 2009). Importantly, each of these v-ATPase mutations is a null or severe loss of function allele, and in none of these mutants are colobomas ever observed. Thus, I hypothesized that $atp6v0b^{N113K}$ was not likely to be a loss of function mutation, and I tested this hypothesis by MO interference. As expected, MO knockdown of *atp6v0b* does not lead to colobomas, and *atp6v0b* morphants do not resemble *blw* mutants (Fig. II-8), rather, they resemble other v-ATPase loss of function mutants (Gross et al., 2005). Additionally, neither injection of *atp6v0b* mRNA or a BAC containing the *atp6v0b* locus into embryos derived from heterozygous *blw* incrosses was able to rescue the *blw* phenotype in these embryos (*data not shown*). Thus, I conclude that $atp6v0b^{N113K}$ is not a loss of function allele.

I also wanted to determine if the $atp6v0b^{N113K}$ mutation might possibly be a gain of function mutation. To test this hypothesis I injected mRNA encoding either

26
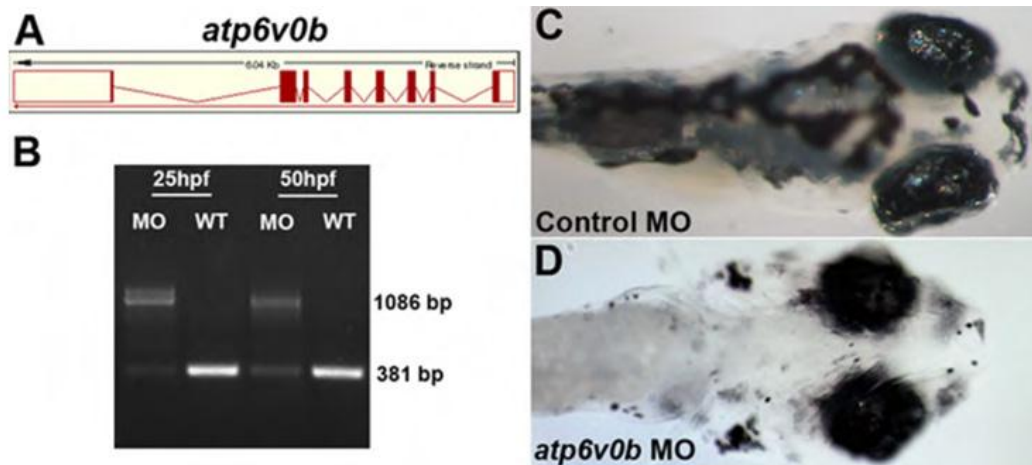
Figure II-8. *atp6v0b* morpholinos do not phenocopy *blowout*.

(A) The *atp6v0b* predicted genomic organization. *atp6v0b* MO targets the exon1/intron1 splice junction and leads to the inclusion of a 705bp intron1 and the introduction of a premature stop codon. (B) RT-PCR validation of splice blocking efficacy of the *atp6v0b* MO. (C) Control injected and (D) *atp6v0b* morphant (13ng) at 5dpf. Morphants display oculocutaneous albinism and retinal degeneration but show no signs of colobomas even at the highest doses of MO injection.

wild-type *atp6v0b* or *atp6v0b^{N113K}* into wild-type 1-cell stage embryos and I assayed

overall eye development and choroid fissure closure through 5dpf. While defects in eye

development were observed that included unilateral microphthalmia, mild to severe

cyclopia and a small percentage of colobomas, their incidence was not significantly

higher in *atp6v0b^{N113K}* injected embryos than those injected with wild-type *atp6v0b*

mRNA (*data not shown*). Thus, while I cannot definitively rule out the hypothesis that

the *atp6v0b^{N113K}* mutation contributes to the colobomas in *blw*, possibly acting as a

modifier locus, neither the results of MO loss of function, mRNA and BAC rescue

assays, nor those testing for gain of function by mRNA overexpression provide

compelling support for this hypothesis.

II. 2. 6. The expression of Hedgehog targets is expanded in *blowout*

Truncation of Patched1 after the 8th transmembrane helix likely prevents it from

inhibiting Smoothened, leading to an expansion of Hh target gene expression in *blw*

mutants. This model is consistent with published reports demonstrating that Hh

overexpression alters gene expression in the optic stalk and optic cup in zebrafish (Ekker

et al., 1995), and consistent with our observations that expression domain of the Shh

target *pax2a*, is expanded in *blw* mutants and *ptc1* morphants, while the *pax6* domain is

contracted (Fig. II-5, Fig. II-7). *ptc1* and *ptc2* are also targets of Hh pathway activation

(Lewis et al., 1999, Concordet et al., 1996), likely acting in a negative feedback

mechanism to limit the diffusion of the Hh morphogen and thus, limit the range of Hh

signaling (Chen and Struhl, 1996). To directly assess whether *ptc1* and/or *ptc2* expression
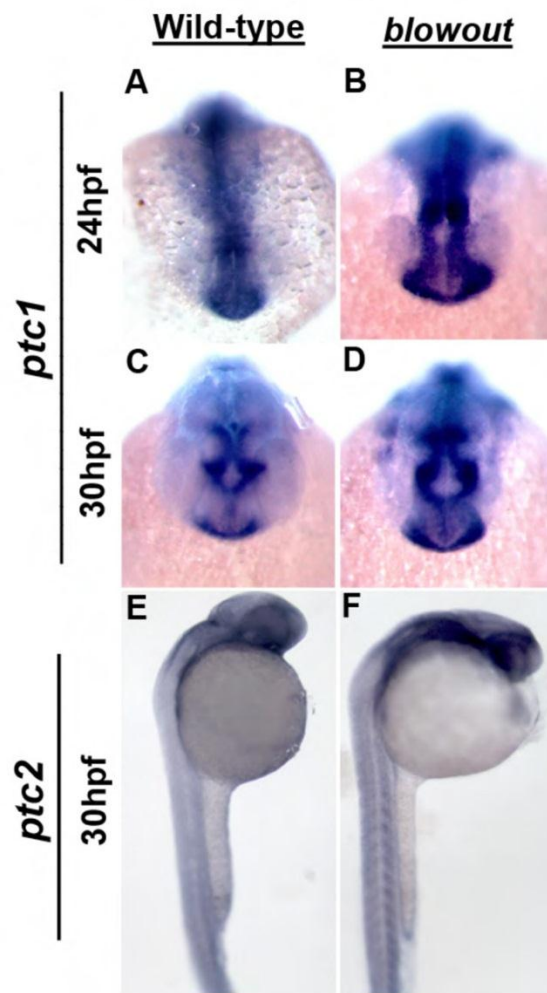
Figure II-9. The domains of the Hh target genes *ptc1* and *ptc2* are expanded in *blowout*.

Expression of *ptc1* in the optic stalk of wild-type embryos at 24hpf (A) and 30hpf (C). (B,D) Expression in *blw* mutants is expanded and appears more intense at these time points both in the optic stalk, as well as in the brain and musculature (*not shown*). *ptc2* expression is also expanded in *blw* mutants (F) relative to wild-type siblings (E).

is altered in *blw*, I assayed their distributions by *in situ* hybridization (Fig. II-9). In wild-type embryos, *ptc1* is strongly expressed in the optic stalk at 24 and 30hpf (Fig. II-9A,C), as well as throughout the ventral brain and the somites (Concordet et al., 1996 and *data not shown*). In *blw* mutants, *ptc1* expression appears to be expanded and the message is distributed in a substantially broader domain of expression (Fig. II-9B,D). Expanded domains of expression were also observed in the ventral brain and the somites (*data not shown*). Similarly, expansion of *ptc1* expression was also observed in *ptc1* morphants (Fig. II-7J,K). Examination of *ptc2* expression in *blw* mutants yielded similar results (Fig. II-9E,F), although changes in *ptc2* distribution were variable in *blw* mutants with only a subset (~40%) showing grossly obvious changes. *ptc2* expression was substantially altered in all *ptc1* morphant embryos (Fig. II-7L,M). I highlight that while *in situ* hybridizations are not quantitative assays, that the *ptc1* and *ptc2 in situ* signals appear to be more intense and expanded in the brain and somites in both *blw* mutant and *ptc1* morphant embryos strongly suggests that Hh pathway activity is upregulated as a result of loss of Patched1 function.

II. 2. 7. Homozygous *blowout* mutants are viable and reveal post-metamorphic roles for Patched1 function in the adult zebrafish

I was able to rear ~2–3% of homozygous *blw* mutant embryos to adulthood and the resulting fish displayed a number of obvious morphological defects (Fig. II-10). *blw* homozygotes were generally smaller in size than their heterozygous and wild-type siblings. Males and females were recovered in approximately equal numbers and fertility

Figure II-10. *blowout* **homozygous adult fish.**

(A,B) blw heterozygous adult fish do not show detectable phenotypes. (C,D) blw homozygous adult fish show jaw defects and kinked bodies.

was normal in the homozygous mutant fish. Embryos derived from homozygous mothers continued to show variable rates of phenotypic penetrance, never reaching predicted Mendelian ratios. On average, the incidence of colobomas was approximately 35% when a homozygous female was mated with a heterozygous male, and incidences rose to over 80% when a homozygous female was mated to a homozygous male. In nearly all mutants derived from homozygous mothers that displayed colobomas, these were almost always observed bilaterally. Importantly, beyond this difference, *blw* mutants derived from homozygous mothers did not show markedly more severe or more widespread developmental defects than those derived from heterozygous mothers, indicating that there is not likely to be a significant maternal mRNA or protein rescue of the *blw* phenotype that masks defects in embryos derived from heterozygous carriers.

II. 2. 8. Is upregulation of Hh pathway activity the mechanism that leads to colobomas in *blowout*?

Given the similarities between Hh overexpression and the *blw* mutation (e.g. changes to *pax2a, pax6, ptc1* and *ptc2* expression), I next sought to directly test the hypothesis that upregulation of Hh pathway activity is the molecular mechanism underlying colobomas in *blw*. To test this hypothesis I utilized cyclopamine, a pharmacological inhibitor of the Hh pathway that acts downstream of Patched (Cooper et al., 1998; Taipale et al., 2002), and asked whether low doses of cyclopamine were capable of suppressing colobomas in *blw* mutants. Indeed, a similar rescue paradigm has been successfully utilized for zebrafish mutations in other negative regulators of the Hh
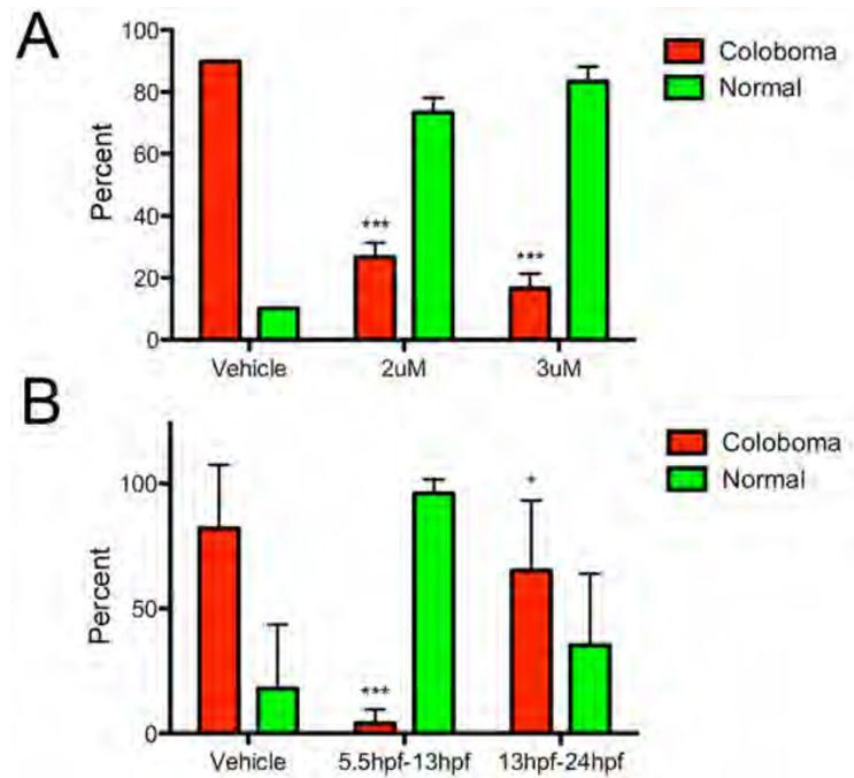
Figure II-11. Cyclopamine suppression of colobomas in *blowout*.

(A) On average, 89.8% of vehicle (EtOH) treated embryos derived from homozygous incrosses displayed colobomas, while exposure of siblings to 2uM or 3uM cyclopamine from 5.5hpf to 24hpf suppressed colobomas to 26.7% and 16.7%, respectively (*** p < 0.0001, Fisher's exact test). (B) Treatment of embryos derived from homozygous incrosses to vehicle (EtOH), or 3uM cyclopamine from 5.5hpf to 13hpf, or 13hpf to 24hpf was also able to suppress colobomas from an average of 82% in vehicle controls to 4% in 5.5–13hpf treated embryos (*** p < 0.0001, Fisher's exact test), and to 65.3% in 13hpf–24hpf treated embryos (* p = 0.0278, Fisher's exact test).

pathway (e.g. *lep/ptc2* and *uki/Hip*; (Koudijs et al., 2005). For these assays, I took advantage of homozygous viable *blw* adults to increase the incidence of coloboma phenotypes and to abrogate the need to genotype each rescued embryo as I knew *a priori* that all were homozygous mutants. Low levels of cyclopamine ($\leq$ 3uM) did not lead to noticeable defects in eye development (*data not shown*) and thus, I assayed whether these subthreshold levels were able to suppress colobomas in *blw*. Exposure of *blw* mutants to 2uM or 3uM of cyclopamine between 5.5hpf and 24hpf was highly effective in suppressing the incidence of colobomas (Figure II-11A). In vehicle treated sibling controls, 89.8% displayed colobomas while 2uM cyclopamine suppressed this to 26.7% and 3uM cyclopamine to 16.7% ($p < 0.0001$; Fisher's exact test).

I next sought to determine if I could identify a window of time between 5.5hpf and 24hpf during which maximal rescue of colobomas in *blw* mutants could be achieved, thereby indicating the window of time when Hh signaling is likely to be required for proximal/distal patterning of the OV during normal embryogenesis. Given that 3uM cyclopamine was able to significantly rescue colobomas in *blw* mutants (Fig. II-11A), I utilized this concentration and exposed embryos over two time windows: 5.5hpf – 13hpf and 13hpf – 24hpf (Fig. II-11B). Maximal rescue was achieved by cyclopamine exposure during the early 5.5hpf – 13hpf window with incidences of colobomas dropping from 82% to 4% ($p < 0.0001$; Fisher's exact test). Cyclopamine exposure from 13hpf – 24 hpf resulted in 65.3% of embryos displaying colobomas ($p = 0.0278$; Fisher's exact test). While the rescue from 13hpf – 24 hpf cyclopamine exposure

is statistically significant when compared to vehicle treated controls, it is substantially lower than that achieved during the early 5.5hpf – 13hpf window of treatment suggesting that it is during this early time window that the Hh signal is normally conveyed to the OV to segregate it into the appropriate proximal and distal territories.

II. 3. DISCUSSION

II. 3. 1. *Blowout* is a loss of function mutation in Patched1

In this study I have characterized zebrafish *blw*, a recessive mutation that presents with ocular coloboma and defects in retinotectal axon pathfinding (Karlstrom et al., 1996). Positional cloning of *blw* identified two mutations; the first of these affects *ptc1*, resulting in a stop codon that truncates the Patched1 protein after the 8th transmembrane domain, and the second affects *atp6v0b*, changing a conserved asparagine residue to a lysine. MO targeting of *ptc1* transcripts results in colobomas while MO targeting of *atp6v0b* transcripts did not lead to colobomas; rather, loss of *atp6v0b* function resulted in oculocutaneous albinism and retinal degeneration. These phenotypes were identical to those observed in six other loss of function mutations in v-ATPase components or v-ATPase associated proteins, suggesting that the *atp6v0b*^{N113K} mutation was not a loss of function allele (Gross et al., 2005; Nuckels et al., 2009). Indeed, neither *atp6v0b* mRNA or BAC injections were able to rescue or alter the ocular defects in *blw* mutants. Additionally, overexpression of *atp6v0b*^{N113K} mRNA did not lead to ocular defects at a higher level than that resulting from overexpression of wild-type *atp6v0b* mRNA, also

35

suggesting that the $atp6v0b^{N113K}$ mutation was not a neomorphic or gain of function allele. Thus, while I cannot exclude the possibility that $atp6v0b^{N113K}$ acts as a modifier of $ptc1^{W1040X}$, our results support a model in which the coloboma phenotypes in *blw* stem solely from a loss of Patched1 function.

Interestingly, *ptc1* morphants showed more severe ocular phenotypes than those observed in *blw* mutants. I was able to rear homozygous mutants to adulthood and embryos derived from incrosses between homozygous parents did not display more severe ocular phenotypes than those derived from heterozygous parents. This indicates that there is not a maternal supply of mRNA or protein that partially rescues the ocular phenotypes in *blw* mutants derived from heterozygous mothers. Phenotypic penetrance varies in clutches of embryos derived from heterozygous parents and while the phenotypic penetrance was higher in clutches derived from homozygous parents, they still never reached predicted ratios. These observations in conjunction with the more severe ocular phenotypes present in *ptc1* morphants, suggest that the ptc^{W1040X} mutation may be a hypomorphic partial loss of function *ptc1* allele.

While direct biochemical analysis of the truncated $Ptc1^{W1040X}$ protein will be required to test this hypothesis, should it retain some of its ability to repress Smoothened, it would be interesting with respect to other mutations that have been identified in the C-terminus of the Patched1 protein. For example, two missense mutations in the human *PATCHED1* (*PTCH*) gene have been identified that alter the C-terminal domain of PTCH (Ming et al., 2002). The first of these mutations resides in the extracellular loop between the 7th and 8th transmembrane domains of PTCH ($PTCH^{T728M}$) and the second resides in

the intracellular loop between the 8th and 9th transmembrane domains of PTCH (PTCH^{T1052M}). Patients with these mutations display holoprosencephaly and other developmental defects, but they do not display colobomas. Interestingly, their phenotypes more closely resemble loss of function mutations in *SONIC HEDGEHOG* (*SHH*) than loss of function mutations in *PTCH*. The biochemical nature of these human mutations have not yet been characterized but given the similarity in phenotypes between them and *SHH* mutations, it may be that they disrupt the portion of the protein that is required for the inactivation of PTCH function in the presence of SHH. Thus, PTCH^{T728M} and PTCH^{T1052M} may act as a dominant negative such that even in the presence of SHH, these mutated proteins still represses SMOOTHENED activity and keep the Hh pathway inactive.

By comparison, truncation of the zebrafish Ptc1 protein at amino acid 1040, between the 8th and 9th intracellular loops, behaves quite differently than these point mutations. In *blw/ptc1* mutants, the Shh pathway appears to be constitutively active although with variable penetrance and relatively milder phenotypes when compared to those that arise from *Shh* overexpression (Ekker et al., 1995). It is possible that the remaining extracellular loop between the 7th and 8th transmembrane domains still retains some of its repressive ability to block Smoothened function when Hh signals are present and thus it is able to ameliorate some of the phenotypes that would be expected to arise if the Hh pathway was fully activated (i.e. to resemble *Shh* overexpression phenotypes). It is also possible that there are other redundant negative regulators of the Hh pathway that prevent full activation of the pathway in *blw/ptc1* mutants, which thereby influence the

37

penetrance of the phenotype. Ptc2 is an ideal candidate to possess a redundant function and indeed, a recent report by Koudijs et al. (2008) demonstrates that the ocular phenotypes in *ptc1/ptc2* double mutants are much more similar to *Shh* overexpression phenotypes than those present in the single mutants.

II. 3. 2. Ptc1-dependent regulation of Hh signaling is required for formation of the optic stalk-retina interface

Shh signaling is a key regulator of proximal OV cell fates (Amato et al., 2004). *pax2a*, a Shh target, has been shown to directly regulate optic stalk and choroid fissure formation in the proximal OV, while *pax6* encodes a key regulatory factor involved in the specification of retina and RPE cell fates within the distal OV (Chow and Lang, 2001; Adler and Canto-Soler, 2007). In the *blw* mutant OV, the early domain of *pax2a* expression is expanded distally and *pax6* expression is contracted (Fig. II-5). These results support a model in which proximal OV cell fates are expanded in *blw* mutants at the expense of distal ones, and this leads to an enlargement of the optic stalk. Indeed, these changes in gene expression in *blw* are identical to those observed from *Shh* overexpression in zebrafish, *Xenopus* and chick (Ekker et al., 1995; Macdonald et al., 1995; Perron et al., 2003; Sasagawa et al., 2002; Zhang and Yang, 2001). One problem with this model however, is that despite the optic stalk expansion and coloboma phenotypes, later aspects of distal OV (i.e. retinal) formation are normal in *blw* mutants. One would expect that if early distal OV patterning were compromised, later retinal and RPE fates would necessarily be affected. This is not the case in *blw* mutants; retinal

patterning is unaffected and overall retina size is similar to that in wild-type siblings. While I do not yet know how distal fates recover in *blw*, one possible mechanism is that the remaining *pax6* expressing distal OV is able to utilize *pax6* in a non-cell autonomous fashion (e.g. Lesaffre et al., 2007), and thereby counteract the effects of the expanded proximal *pax2a* expressing regions. In this scenario, the optic stalk would be refractory to this "rescue" and thus still expand into the choroid fissure, but the remainder of the distal OV is able to develop relatively normally. Additional analyses are required to test this hypothesis and to determine why *blw* mutants do not display distal OV defects despite the early changes in gene expression domains observed within the OV at 18hpf.

Colobomas in *blw* were suppressed by pharmacological inhibition of Hh pathway activity indicating that it is dysregulation of this pathway that underlies the coloboma phenotype. I suspect that colobomas result from the expansion of the optic stalk into the choroid fissure which prevents its lateral edges from meeting and fusing, however it is also possible that overproliferation of cells within the optic stalk itself contributes to these colobomas by further expanding the optic stalk into the ventral optic cup, and thus impeding its closure. Hh signaling is known to regulate cell proliferation in a number of cellular and developmental contexts, including the eye, through the activation of key cell cycle regulators like cyclin D1, cyclin B1 and cyclin A2, as well as the phosphatase, Cdc25, that collectively function to maintain proliferative cells in the cell cycle (Adolphe et al., 2006; Agathocleous et al., 2007; Locker et al., 2006). In *blw*, a Hh dependent dysregulation of cell proliferation may also be occurring within the proximal OV which increases the amount of stalk tissue and thereby physically impedes closure of the

choroid fissure. It will be interesting in future studies to determine if proliferation and the expression of these cell cycle components are upregulated in the optic stalk of *blw* mutants.

Hh signaling is required for later aspects of optic stalk development in mouse whereby retinal ganglion cell derived Shh is required for optic stalk neuroepithelial cells to develop into astroglia, as well as to suppress pigment cell formation around the optic nerve (Dakubo et al., 2003; Torres et al., 1996). I observed continued expression of *pax2a* mRNA in the optic stalk and ectopically in the retina of *blw* mutants when compared to that in wild-type siblings, where expression had ceased and differentiation commenced by 48hpf. Beyond the coloboma induced morphological abnormalities in the retina of *blw* mutants, histologically and immunohistocehmically their retinas appear relatively normal. That said, I do not know the effect of the mutation on later aspects of optic stalk development, as I have not yet assayed the differentiated state of the optic stalk in *blw* mutants. Based on the results in mouse, one might hypothesize that neuroepithelial cells of the *blw* optic stalk would remain undifferentiated due to the prolonged expression of these specification genes. Conversely, one might also hypothesize that the optic stalk in *blw* might differentiate but that glial cells would be overrepresented as a result of dysregulated Hh target gene expression. *blw* was originally identified based on defects in retinotectal pathfinding (Karlstrom et al., 1996), and in either of the above scenarios, retinal ganglion cell axons would likely not properly find their way to the optic nerve and/or the optic tectum. Future studies will be required to

40

examine these possibilities and determine the molecular basis for the pathfinding defects in *blw*.

Finally, underscoring the importance of Patched dependent regulation of Hh signaling in human disease, loss of function mutations in human *PTCH* lead to Basal Cell Naevus or Gorlin syndrome (BCNS; OMIM #109400), a developmental disorder characterized by dental, skeletal and ocular defects (Hahn et al., 1996; Johnson et al., 1996). Ocular phenotypes associated with BCNS include abnormal myelination of the optic nerve, retinal dysplasia and colobomas; however, the mechanism through which *PTCH* mutations lead to these ocular defects has not been established (Black et al., 2003; De Jong et al., 1985; Manners et al., 1996). Our results demonstrate a critical role for zebrafish Patched1 in negatively regulating Hedgehog signaling within the proximal OV and possibly in functioning to restrict Hh-dependent cell proliferation therein. BCNS-related pathologies may result from unrestricted proliferation within the retina, a model recently proposed by Black et al. (2003). That a subset of homozygous adult *blw* mutants are viable will enable us to test this hypothesis and to identify later roles for *ptc1*-dependent Hh regulation in ocular development and homeostasis, as well as to model other non-ocular BCNS associated pathologies in zebrafish.

CHAPTER III

FUNCTION AND REGULATION OF BCL6 DURING ZEBRAFISH EYE DEVELOPMENT

III. 1. INTRODUCTION – Bcl6 (B cell leukemia/lymphoma 6) Protein

III. 1.1. Regulation of Bcl6

The human proto-oncogene *BCL6* (B cell leukemia/lymphoma 6) encodes a sequence-specific transcriptional repressor (Chang et al., 1996; Seyfert et al., 1996). *BCL6* was originally studied based on its involvement in certain types of lymphomas, in which *BCL6* expression is deregulated (Baron et al., 1993; Kerckaert et al., 1993; Ye et al., 1993). Chromosomal translocations affecting band 3q27 were found to deregulate *BCL6* expression by a promoter substitution putting heterologous promoters adjacent to the *BCL6* coding region (Ohno, 2004; Pasqualucci et al., 2003; Ye et al., 1995). Lymphomas with deregulated BCL6 expression were found to contain somatic point mutations in the 5' non-coding region of *BLC6* (Migliazza et al., 1995). From the study of lymphomas, it appears likely that BCL6 expression is strictly regulated during differentiation of B cells. Indeed, BCL6 is not detectable in pre-germinal center B cells, but is exclusively expressed in germinal center B cells, and this expression is not observed in differentiated plasma B cells (Cattoretti et al., 1995; Flenghi et al., 1995; Onizuka et al., 1995). *BCL6* is transcriptionally down-regulated by signaling induced by

CD40 receptors (Allman et al., 1996). BCL6 also can be regulated at the protein level; phosphorylation mediated by MAP kinase targets BCL6 for degradation when antigens bind to B cell receptors (Niu et al., 1998).

III. 1.2. Function of Bcl6

BCL6 is known to be important for germinal-center formation in mouse (Dent et al., 1997). In germinal-center B cells, BCL6 plays an important role in circumventing apoptotic responses from DNA breaks for immunoglobulin class switch recombination by directly suppressing the expression of *p53* tumor suppressor gene (Phan and Dalla-Favera, 2004). Furthermore, in the olfactory system, BCL6 functions as an anti-apoptotic factor providing enough time for olfactory sensory neurons to differentiate into mature neurons in mouse (Otaki et al., 2010). While the involvement of BCL6 in B cell development and lymphomagenesis has been well studied, its functions during embryonic development remain poorly elucidated. Recently, BCL6 has been reported to be involved in the patterning of left-right asymmetry by inhibiting Notch target genes, thus maintaining the expression of *Pitx2* in the left lateral plate mesoderm in *Xenopus* (Sakano et al., 2010).

BCL6 is known to have three functional domains, including a POZ/BTB domain at the N terminus, a central repression domain, and a zinc finger motif at the C terminus (Bardwell and Treisman, 1994; Stogios et al., 2005; Zollman et al., 1994). Through the POZ/BTB domain BCL6 interacts with several corepressors, including BCL6 corepressor (BCOR), SMRT (silencing mediator of retinoic acid and thyroid hormone receptor), and

NCOR (nuclear receptor corepressor) to silence genes involved in apoptosis and cell cycle arrest (Huynh et al., 2000; Polo et al., 2004). The central repression domain of BCL6 is involved in associating with a corepressor, metastasis-associated protein 3 (MTA3) and a HDAC-containing chromatin remodeling complex, Mi-2/NuRD, in order to suppress genes responsible for plasma cell differentiation (Fujita et al., 2004; Polo et al., 2004). The six Cys2-His2 zinc finger motif plays a role in recognizing specific DNA squences (Kawamata et al., 1994).

III. 1.3. Cofactors of Bcl6

III. 1.3.1. Bcor (Bcl6 co-repressor)

BCOR is a corepressor that potentiates transcriptional repression by BCL6 (Huynh et al., 2000). Different types of mutations in *BCOR* have been found in patients with Oculofaciocardiodental (OFCD; OMIM 300166) syndrome, which is an X-linked male lethal condition displaying ocular defects (coloboma), cardiac septal defects, and dental anomalies (Gorlin et al., 1996; Hedera and Gorski, 2003; Ng et al., 2004; Schulze et al., 1999). Knock-down of BCOR in zebrafish and *Xenopus* embryos recapitulates the human syndrome with developmental disruption of the eye including colobomas and defects in the skeleton and central nervous system, suggesting that BCOR plays multiple critical roles in the development of different organs (Hilton et al., 2007; Ng et al., 2004). BCOR is part of a transcriptional repression complex containing Ring finger protein 2 (RNF2), an E3 ligase that ubiquitinates histone H2A, which is known to keep chromatin in a repressed state (Cao et al., 2005; de Napoles et al., 2004; Jason et al., 2005; Wang et

al., 2004). FBXL10/JHDM1B, an F-box protein with a JmjC demethylase domain, also belongs to the BCOR complex. It is known to demethylate histone H3K36 demethylation (Tsukada et al., 2006), known as a silencing mechanism (Bannister et al., 2005; Rao et al., 2005). These studies suggest that BCOR functions to silence genes through a combination of epigenetic modifications (Gearhart et al., 2006). The BCOR complex is recruited by BCL6 to target genes including *p53* and *cyclin D2* to potentiate transcriptional repression in B cells (Gearheart et al., 2006). BCOR is critically involved in the patterning of left-right asymmetry by maintaining the expression of *xtPitx2c* in the left side of *Xenopus* embryos, similar to BCL6 (Hilton et al., 2007; Sakano et al., 2010), indicating that BCOR acts as a corepressor for BCL6 in left-right patterning as well.

III. 1.3.2. Hdac1 (Histone deacetylase 1)

Acetylation is thought to activate transcription by modifying histones (Sterner and Berger, 2000) or by directly regulating activity of transcription factors like E2F and p53 (Barlev et al., 2001). Furthermore, acetylation of transcriptional repressors, like BCL6, is also inhibitory, providing a third mechanism by which acetylation can stimulate transcription (Bereshchenko et al., 2002). Bereshchenko et al. demonstrated that HDACs play an important role in regulating Bcl6 activity by controlling its acetylation state. BCL6 is known to require association with complexes containing HDACs and co-repressors to function as a transcriptional repressor (Dhordain et al., 1997; Dhordain et al., 1998; Wong and Privalsky, 1998). In zebrafish, *hdac1* mutation results in colobomas (Stadler et al., 2005; Yamaguchi et al., 2005). In *hdac1* mutants, retinal cells fail to exit

the cell cycle and don't differentiate into neurons and glial cells, suggesting that Hdac1 promotes cell cycle exit and differentiation of retinal cells. In retinal cell culture, inhibition of Hdac function by trichostatin A (TSA) induces expression of Apaf-1, a pro-apoptotic protein, by increasing expression of upstream regulators like *p53*, suggesting that Hdac activity is involved in regulating apoptosis in the retina (Wallace and Cotter, 2009; Wallace et al., 2006).

Here, I propose that Bcl6 plays a critical role in preventing apoptosis in the retina during eye development, and that this function is required to contain the retina and RPE within the optic cup. In addition, I suggest that Vax1 and Vax2 act upstream of *bcl6* in the ventral retina, and Bcl6 functions along with Bcor and Hdac1 to mediate cell survival by regulating *p53* within the developing zebrafish retina.

III. 2. RESULTS

III. 2. 1. *bcl6* is expressed in the ventral retina.

To investigate when and where *bcl6* is expressed during zebrafish eye development, I examined the expression pattern of *bcl6* mRNA by *in situ* hybridization with *bcl6* anti-sense ribo-probe at several different time points on wild type embryos. *bcl6* was expressed in the lens and myotome prior to 24 hpf and disappeared after 24 hpf (data not shown). In the retina, *bcl6* started to be expressed in the choroid fissure at 30 hpf, and this expression domain began to expand into the nasal retina at 39 hpf (Figs. III-

1A-C). Transcripts expanded both nasally and temporally in the outermost region of the retina by 48 hpf and eventually *bcl6* was detected in most of the ventral retina at 54 hpf (Figs. III-1D-F). *bcl6* is also detected in the optic tectum after 39 hpf (Figs. III-1G,H).

III. 2. 2. Vax1 and Vax2 regulate the expression of *bcl6* in the ventral retina.

It has been reported that Vax1 and Vax2 are expressed in the optic stalk and ventral retina during early eye development when they regulate transcription of target genes involved in eye development. Moreover, loss of Vax1 and Vax2 function results in colobomas in mouse and zebrafish (Take-uchi et al., 2003). To investigate if *bcl6* expression is regulated by Vax1 and Vax2 in the retina, I co-injected 3.8ng of *vax1* MO and 3.8ng of *vax2* MO (Take-uchi et al., 2003), and examined *bcl6* expression at 48 hpf by *in situ* hybridization. *bcl6* was not detected in the retina of *vax1/vax2* morphants, while *bcl6* was expressed in the ventral retina of control morpholino (con-MO) injected embryos (Figs. III-2A,B). These results indicate that Vax1 and Vax2 likely act upstream of *bcl6* in the ventral retina.

III. 2. 3. Knock-down of Bcl6 causes colobomas in zebrafish and *Xenopus*.

To determine the function of Bcl6 in the developing eye, I performed a knock-down analysis by injecting 7.5ng of a splice-blocking morpholino (*bcl6*-MO) targeting the *bcl6* transcript. Knock-down of Bcl6 resulted in colobomas which were detected at 2 dpf and obvious at 3 dpf, while 5 base-pair mismatch morpholino (*bcl6*-MMO) injected embryos developed normally (Figs. III-3D-I). *bcl6*-MO injected embryos also had curved

47
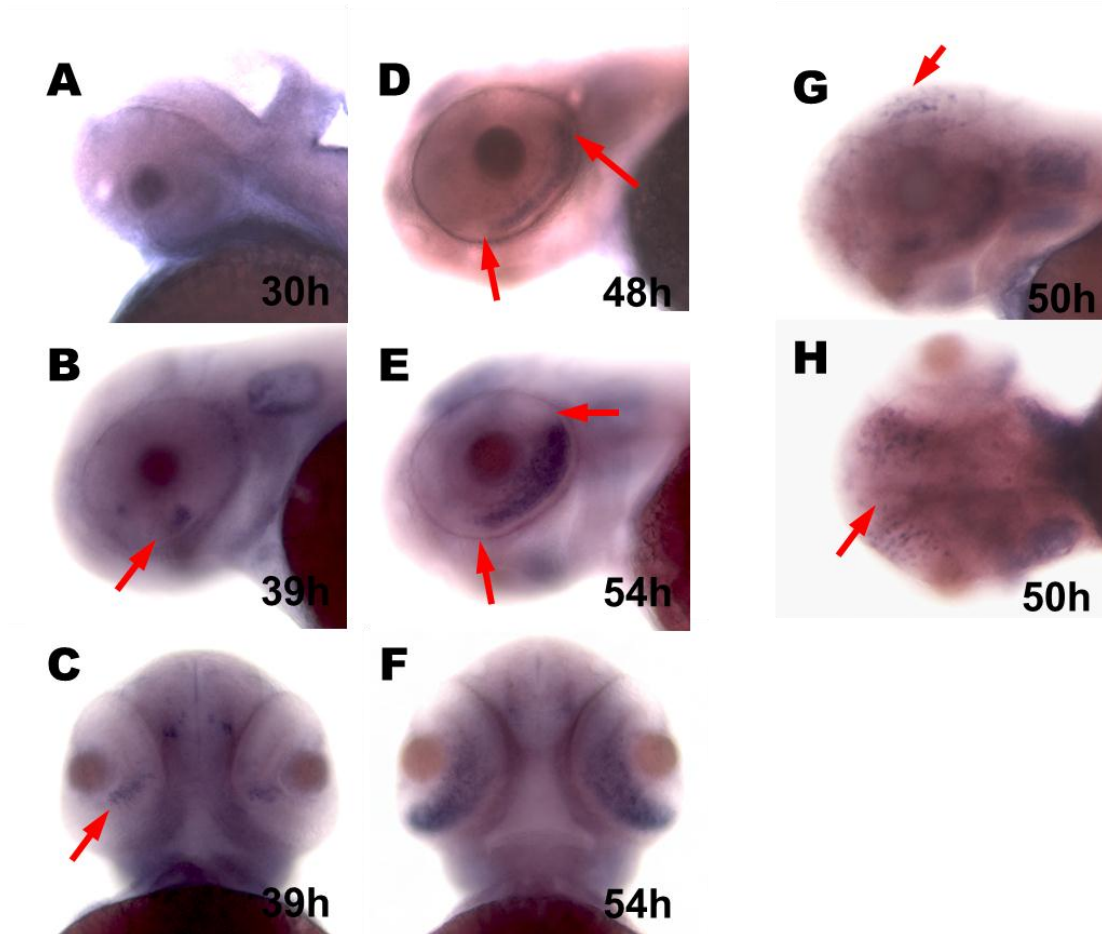
Figure III-1. Expression pattern of *bcl6* in the zebrafish eye.

bcl6 expression in the retina of wild-type embryos at (A)30 hpf, (B,C) 39 hpf, (D) 48 hpf, and (E,F) 54 hpf imaged (A,B,D,E) laterally and (C,F) ventrally. (A) *bcl6* expression is observed in the choroid fissure at 30 hpf, and (B-F) later expands into the ventral retina. *bcl6* expression in the optic tectum at 50 hpf imaged (G) laterally and (H) dorsally. Dorsal is up in panels A,B,D,E,G. Anterior is up in panels C,F.
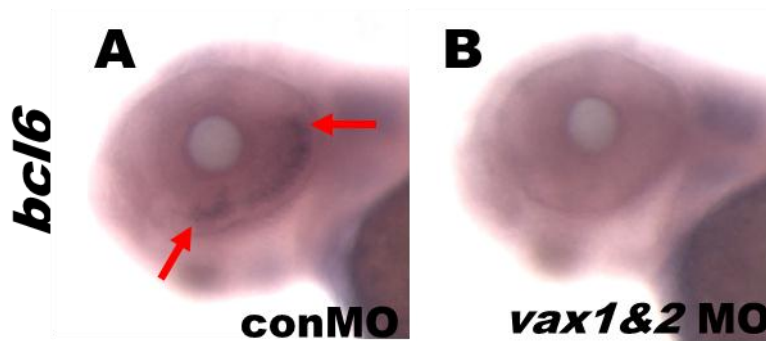
Figure III-2. Vax1 and Vax2 regulate the expression of *bcl6* in the ventral retina.

bcl6 expression in (A) con-MO injected embryos and (B) *vax1&vax2* morphants at 48 hpf imaged from the lateral side. *bcl6* is not detected in the retina of *vax1&vax2* morphants.

Figure III-3. Knock-down of Bcl6 causes colobomas in zebrafish (3 dpf).

(A,D,E) *bcl6*-MMO and (B,C,F-I) *bcl6*-MO injected embryos at 3 dpf imaged (A-D,F,H) laterally and (E,G,I) ventrally. Transverse histological sectioning of (J) *bcl6*-MMO and (K) *bcl6*-MO injected embryos. 7.5ng injection of *bcl6*-MO targeting *bcl6* transcript resulted in (A-C) curved bodies and (D-K) colobomas. Dorsal is up in panels A-D,F,H,J,K. Anterior is up in panels E,G,I.

bodies, suggesting that Bcl6 expressed in the somites may be required for trunk formation (Figs. III-3A-C). Histological analysis confirmed colobomas in *bcl6*-MO injected embryos, with retinal tissue protruding into the forebrain. Retinal lamination, and lens and RPE formation were normal, and all retinal cell types were present in the *bcl6*-MO injected embryos (Figs. III-3J,K). By 5dpf, colobomas in *bcl6*-MO injected embryos were more severe, with *bcl6* deficient embryos possessing large holes in the posterior of the eye with an extrusion of retinal and RPE tissue (Figs. III-4A-F).

To confirm that colobomas in *bcl6*-deficient embryos resulted from specific roles for Bcl6 in eye development, I designed and injected 7.5ng of a 2nd morpholino that targeted the translation start site of *bcl6* (*bcl6*-MO2). *bcl6*-MO2 injected embryos also presented with colobomas, along with defects in trunk formation, and phenocopied the *bcl6*-MO injected embryos (data not shown). To further confirm that the colobomas in the *bcl6*-MO and *bcl6*-MO2 injected embryos are a specific phenotype from knock-down of Bcl6, I performed co-injection of *bcl6*-MO and *bcl6*-MO2 at sub-optimal levels (i.e. those that do not lead to a coloboma when injected alone). When I reduced the injection amount of *bcl6*-MO from 7.5ng to 2.5ng, no injected embryos showed colobomas or trunk defects. Similarly, when *bcl6*-MO2 was injected at 2.5ng/embryo, development was normal. However, co-injection of 2.5ng *bcl6*-MO and 2.5ng *bcl6*-MO2 resulted in colobomas in all injected embryos (n=23) (Figs. III-5A-F).

To determine if Bcl6 function in the eye is conserved in other vertebrates, I applied knock-down analysis of Bcl6 in *Xenopus laevis*. When I injected 40ng of a translation blocking morpholino (*xbcl6*-MO) targeting *Xenopus bcl6* transcripts into one

51

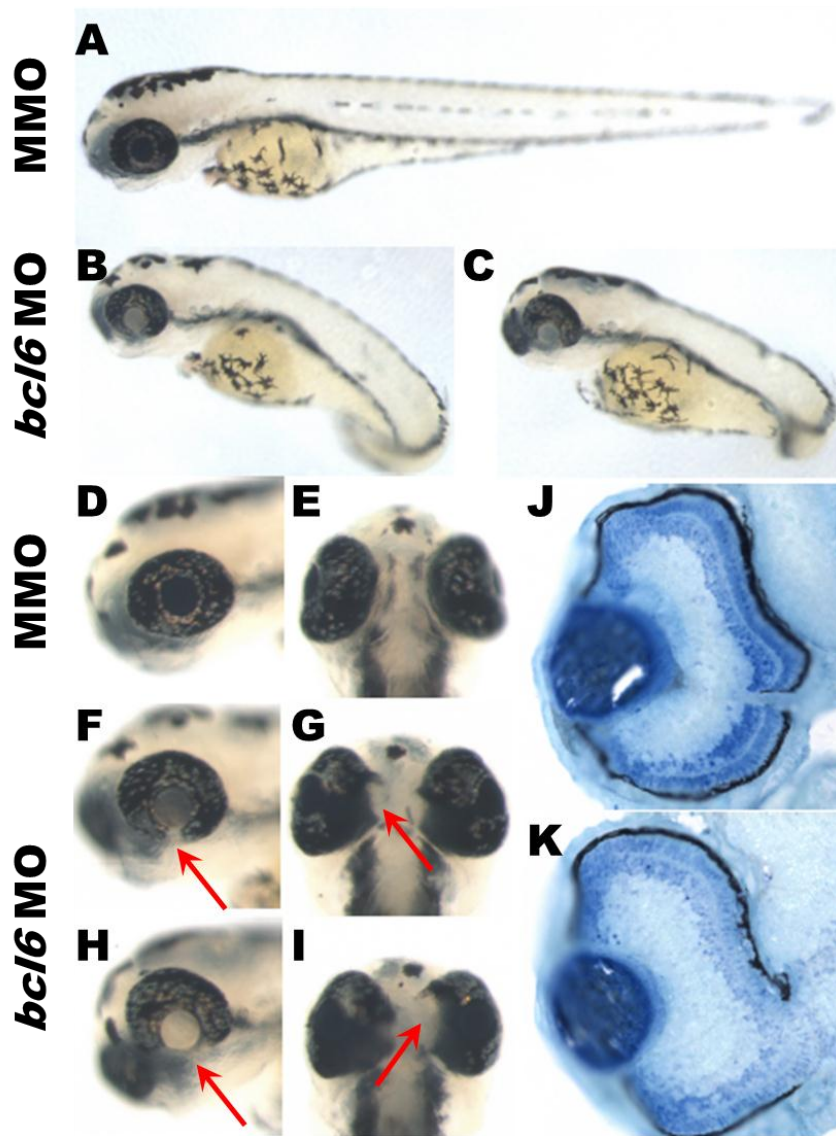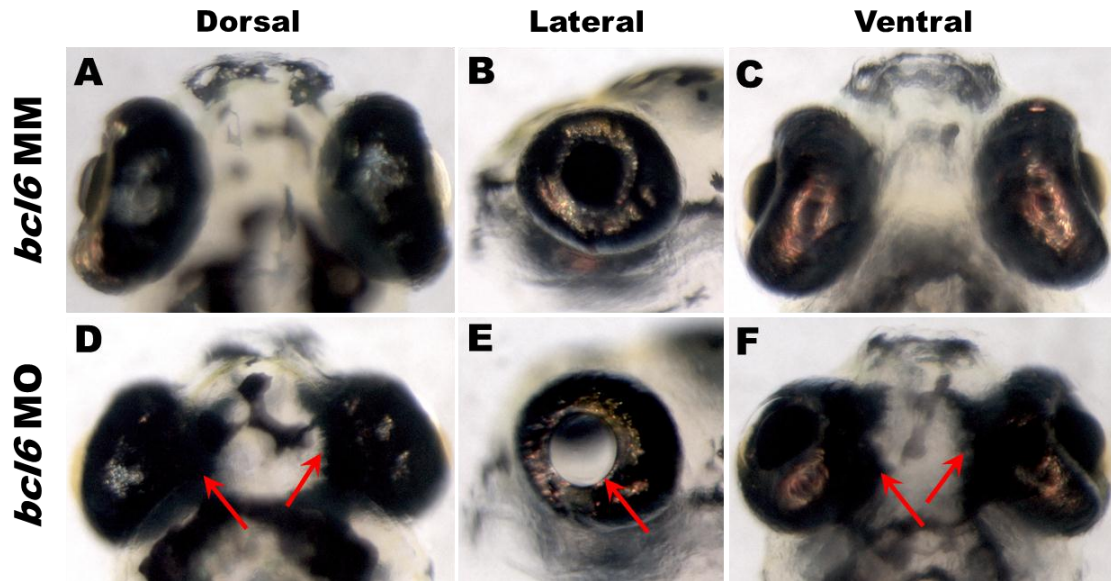**Figure III-4. Knock-down of Bcl6 causes colobomas in zebrafish (5 dpf).**

(A-C) *bcl6*-MMO and (D-F) *bcl6*-MO injected embryos at 5dpf imaged (A,D) dorsally, (B,E) laterally and (C,F) ventrally. By 5dpf, (D-F) colobomas in *bcl6*-MO injected embryos are more severe, with *bcl6* deficient embryos possessing large holes in the posterior of the eye and an extrusion of retinal and RPE tissue. Anterior is up in panels A,C,D,F. Dorsal is up in panels B,E.
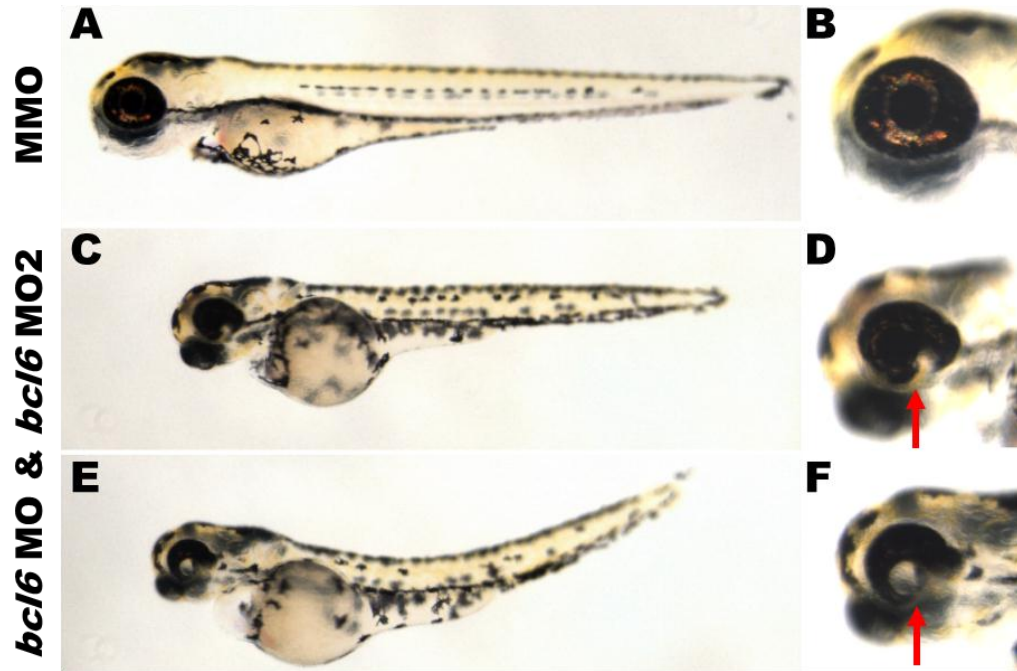
Figure III-5. Knock-down of Bcl6 causes colobomas in zebrafish.

(A,B) *bcl6*-MMO and (C-F) *bcl6*-MO & *bcl6*-MO2 injected embryos at 3 dpf were imaged laterally. Co-injection of 2.5ng *bcl6*-MO and 2.5ng *bcl6*-MO2 resulted in colobomas (arrows in panels D,F). Dorsal is up in all images.

of dorsal cells at 4-cell stage, the injected side in 76% of *xbcl6*-MO injected embryos (n=25) showed colobomas and extrusion of retinal and RPE tissue into the forebrain, phenocopying colobomas in *bcl6*-MO injected zebrafish embryos (Figs. III-6A-F). Eye development from the un-injected side was normal. These results demonstrate that bcl6 is required for normal eye development in both zebrafish and *Xenopus* embryos

III. 2. 4. Bcl6 prevents cell death by suppressing *p53* expression in the retina.

It has been reported that human BCL6 is involved in preventing apoptosis from hypermutation and chromosome rearrangement in germinal center B cells (Phan & Dalla-Favera, 2004). To test if Bcl6 prevents apoptosis in the retina, acridine-orange staining was used to detect apoptotic cells in *bcl6*-MMO and *bcl6*-MO injected embryos at 48 hpf, a time at which there are typically no apoptotic cells in the retina of wild-type embryos (Cole and Ross, 2001). Indeed, *bcl6*-MMO injected retinas possessed no apoptotic cells (100%, n=22), while there were numerous apoptotic cells in the retinas of *bcl6*-MO injected embryos (71%, n=35) (Figs. III-7A,B), indicating that knock-down of Bcl6 resulted in increased cell death in the retina.

Given that BCL6 in germinal center B cells directly suppresses *p53* expression in order to control apoptosis (Phan & Dalla-Favera, 2004), I investigated if Bcl6 also plays a role in regulating *p53* expression to prevent apoptosis in the developing retina by examining *p53* expression at 48 hpf through *in situ* hybridization. While *p53* expression was nearly absent in the eye of *bcl6*-MMO injected embryos, there was an expansion of *p53* in the retina of *bcl6*-MO injected embryos (Figs. III-7C,D). As well, *p53* expression
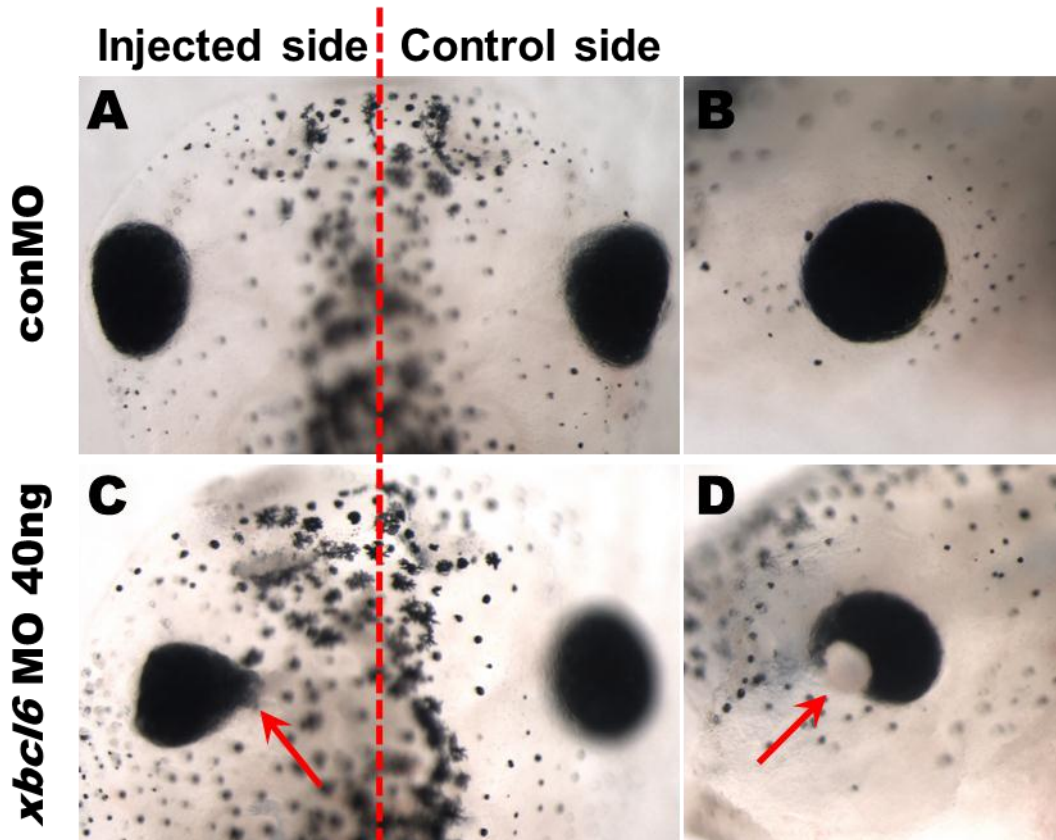
Figure III-6. Knock-down of Bcl6 causes colobomas in *Xenopus*.

(A,B) con-MO and (D-F) a translation blocking morpholino targeting *Xenopus bcl6* transcripts (*xbcl6*-MO) injected *Xenopus* embryos at stage 41 were imaged (A,C) dorsally and (B,D) laterally. 40ng injection of *xbcl6*-MO results in colobomas, (A,C) an extrusion of retinal and RPE tissue, and (B,D) a lack of a large part of the ventral retina. Injected side is left in panels A,C. Anterior is up in panels A,C. Dorsal is up in panels B,D.
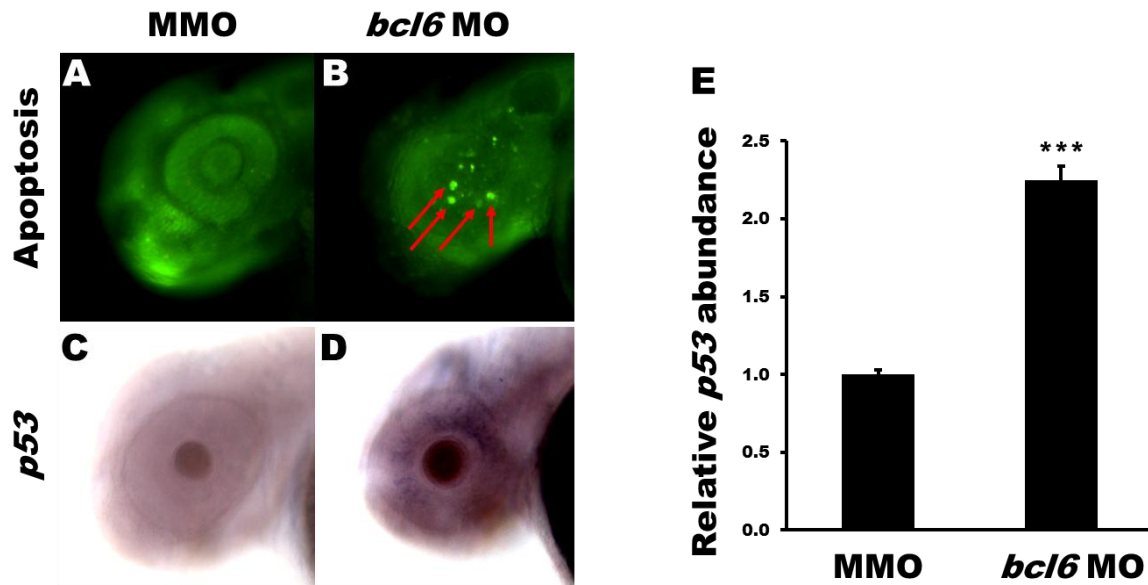
Figure III-7. Knock-down of Bcl6 resulted in increased apoptotic cells along with increased *p53* expression in the retina.

Acridine orange staining in (A) *bcl6*-MMO and (B) *bcl6*-MO injected embryos at 48 hpf. Bcl6 deficient embryos present with increased number of apoptotic cells in the retina (arrows in panel B). *p53* expression in (C) *bcl6*-MMO and (D) *bcl6*-MO injected embryos at 48 hpf. *p53* expression domain is observed in the retina and tectum. (E) Quantitative anaylsis by qRT-PCR shows 2.3 fold increase of *p53* levels in *bcl6*-MO injected embryos.

expanded in the tectum (Fig. III-7D), a region that also expresses *bcl6* at 48 hpf (Fig. III-1G,H). To quantify *p53* expression, qRT-PCR was performed on mRNA isolated from *bcl6*-MMO and *bcl6*-MO injected embryos. Comparison of *p53* levels between *bcl6*-MMO and *bcl6*-MO injected embryos after normalization by *b-actin* indicated that *p53* level in *bcl6*-MO injected embryos was 2.3 times higher than that in *bcl6*-MMO injected embryos ($p<0.0001$; t Test) (Fig III-7E).

To determine if increased *p53* levels were responsible for colobomas in *bcl6*-MO injected embryos, a rescue experiment was performed via knock-down of p53 with concurrent knock-down of Bcl6. Co-injection of 7.5ng *bcl6*-MO and 7.5ng *bcl6*-MMO (as a "load" control) resulted in colobomas along with curved bodies as in previous experiments (Figs. III-8A,B,D-G). Co-injection of 7.5ng *bcl6*-MO with 7.5ng *p53* morpholino (*p53*-MO) rescued colobomas and trunk formation (n=25) (Figs. III-8C,H,I), indicating that increased *p53* expression may underlie colobomas in Bcl6-deficient embryos. These results suggest that Bcl6 functions as a regulator of apoptosis by controlling *p53* expression in the developing eye and that Bcl6-dependent repression of *p53* is required for normal eye development.

III. 2. 5. Vax1 and Vax2 regulate *bcl6* expression in the retina.

Given that Vax1 and Vax2 induce the expression of *bcl6* in the ventral retina (Figs. III-2A,B), I investigated whether *vax1/vax2* morphants present with molecular phenotypes as well as colobomas similar to *bcl6*-MO injected embryos. First, *p53* expression was examined by *in situ* hybridization. There was an increase of *p53*

57
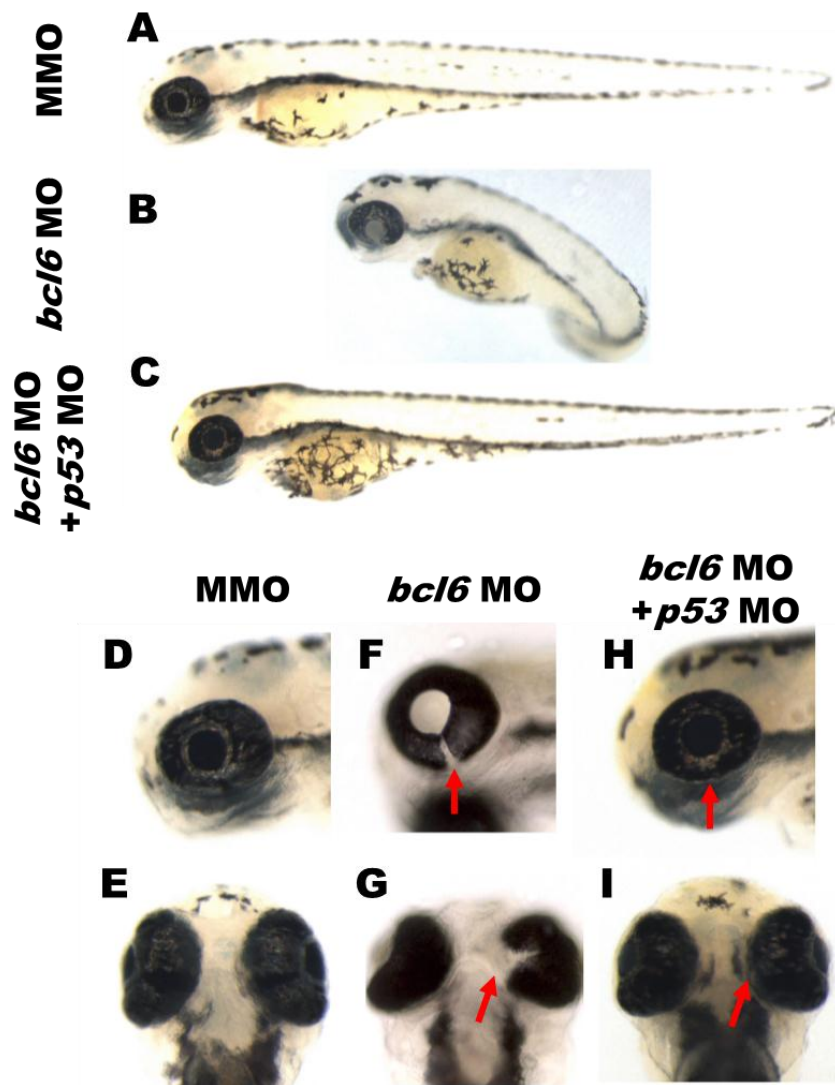
Figure III-8. Co-knock-down of p53 suppresses colobomas in *bcl6*-MO injected embryos.

(A,B,D-G) *bcl6*-MO injected embryos present with colobomas (arrows in panels F,G) and (B) curved bodies at 3 dpf. (C,H,I) Co-injection of *p53*-MO with *bcl6*-MO suppresses colobomas (arrows in panels H,I) and defects in trunk formation.

expression in the retina of *vax1*/*vax2* morphants at 48 hpf, while *p53* expression was nearly absent in the eye of con-MO injected embryos (Figs. III-9A,B). To confirm the increased *p53* expression with a quantitative analysis, qRT-PCR was performed on con-MO injected embryos and *vax1*/*vax2* morphants. After normalization to *β-actin* levels, *p53* expression levels in *vax1*/*vax2* morphants were 4.4 times higher than that in con-MO injected embryos (p<0.0001; t Test) (Fig. III-9C), supporting *in situ* hybridization results. Secondly, I performed acridine-orange staining to detect apoptotic cells in the retina of *vax1*/*vax2* morphants at 48 hpf. There was an increase in the number of apoptotic cells in the retina of *vax1*/*vax2* morphants (68%, n=19), compared to that in con-MO injected embryos, which showed no apoptotic cells (100%, n=21) (Figs. III-9D,E). As previously reported, *vax1*/*vax2* morphants also present with colobomas (Take-uchi et al., 2003); histological analysis confirmed the coloboma phenotype, revealing missing ventral retina tissue and holes in the posterior of the eyes (Figs. III-9H,I,K,L). These results demonstrate that knock-down of Vax1 and Vax2 results in a similar molecular phenotype to knock-down of Bcl6, including colobomas. To test if the increase in *p53* expression in *vax1*/*vax2* morphants is responsible for the increase of apoptotic cells and colobomas, I performed rescue experiments by co-knock-down of p53 along with knock-down of Vax1 and Vax2. Interestingly, co-knock-down of p53 rescued the increased apoptotic cells as well as the coloboma phenotype (86%, n=22) (Figs. III-9F,J,M). These results support a model that Vax1 and Vax2 function as upstream regulators of *bcl6* in order to control apoptosis by suppressing *p53* expression in the developing eye.
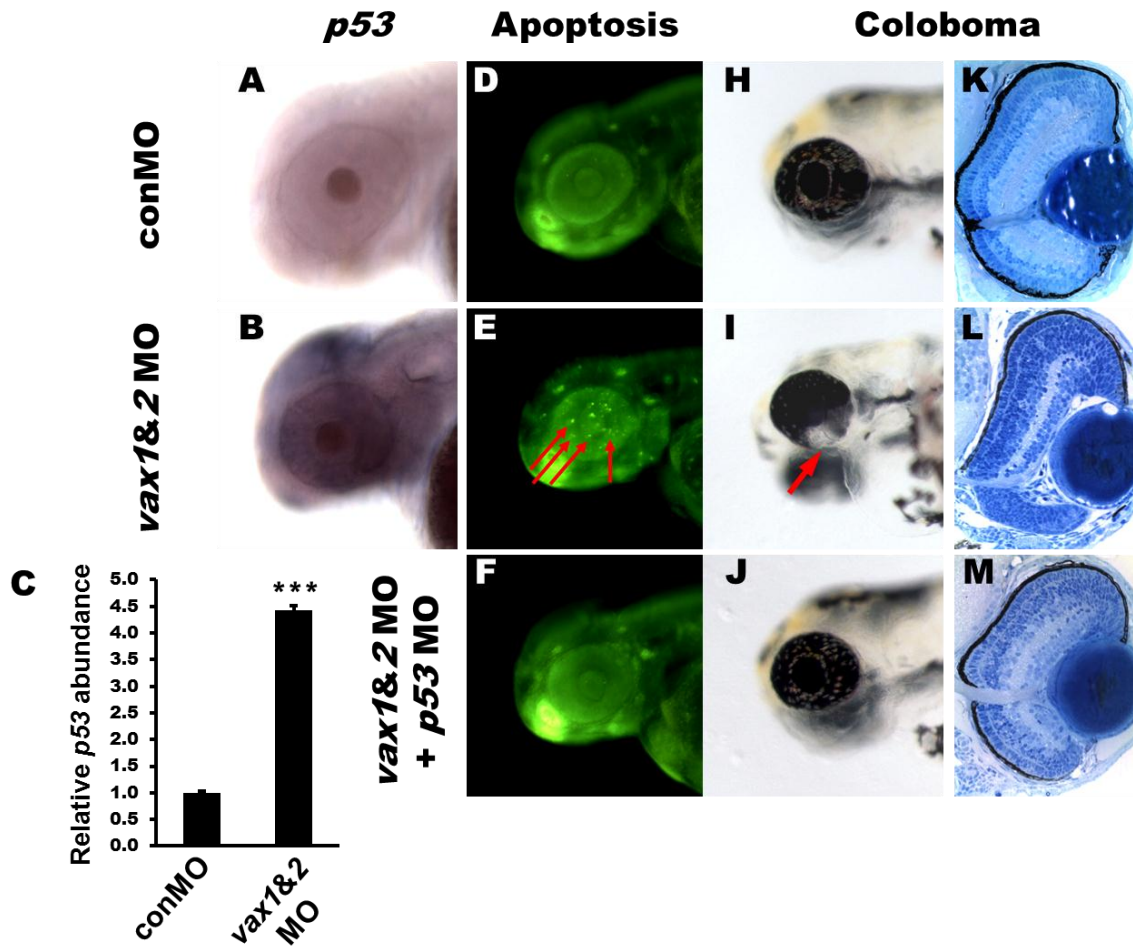
Figure III-9. Vax1 and Vax2 regulate *bcl6* expression in the retina.

p53 expression in (A) con-MO and (B) *vax1&2*-MO injected embryos at 48 hpf. (A,B) There is an increase of *p53* expression in the retina of *vax1&2*-MO injected embryos, while *p53* expression is nearly absent in the eye of con-MO injected embryos. (C) Quantitative anaylsis by qRT-PCR shows 4.4 fold increase in *p53* levels in *vax1/vax2* morphants. Acridine orange staining in (D) con-MO and (E) *vax1&2*-MO injected embryos at 48 hpf. Vax1&2 deficient embryos present with an increased number of apoptotic cells in the retina (arrows in panel E). (G,I) Knock-down of Vax1 and Vax2 results in colobomas. (K,L) Transverse histological sectioning of *vax1&2*-MO injected embryos at 3 dpf shows extrusion of retinal tissue and RPE. (F) Co-knock-down of p53 inhibits apoptosis in *vax1&2*-MO injected embryos. (J,M) Colobomas is suppressed by co-injection of *p53*-MO with *vax1&2*-MO.

III. 2. 6. Bcor and Bcl6 functionally interact in the eye.

It has been shown that several co-factors are required for Bcl6 to function as a transcriptional repressor (Dhordain et al., 1997; Dhordain et al., 1998; Wong and Privalsky, 1998), one of which is Bcor, a Bcl6 co-repressor. Bcor has been reported to be mutated in OFCD syndrome, a human disorder in which some patients present with colobomas (Ng et al. 2004; Hilton at al., 2007), and functional studies in *Xenopus* and zebrafish also support a role in suppressing colobomas (Ng et al. 2004; Hilton at al., 2007). To test if knock-down of Bcor results in a similar phenotype on the molecular level to knock-down of Bcl6, *p53* expression and apoptosis were examined in Bcor knock-down embryos. Following injection of 1ng of splice blocking morpholino targeting exon12/intron12 of *bcor* (*bcor*-MO), *p53* expression was analyzed by *in situ* hybridization and qRT-PCR, and histological analysis was performed to determine morphological effects. While *p53* expression was nearly absent in the eye of con-MO injected embryos, there was a marked increase of *p53* expression in the retina of *bcor-MO* injected embryos at 48 hpf (Figs. III-10A,B). qRT-PCR data revealed a 5.4 fold increase of *p53* expression in *bcor*-MO injected embryos compared to that in con-MO injected embryos ($p<0.0001$; t Test) (Fig. III-10E). Acridine orange staining at 48 hpf demonstrated numerous scattered apoptotic cells in the retina of *bcor*-MO injected embryos, while no apoptotic cells were detected in the retina of con-MO injected embryos (Figs. III-10C,D). Whole mount imaging and histological analyses of *bcor*-MO injected embryos revealed severe colobomas, where a large part of the ventral retina was missing (Figs. III-10F-K). These results demonstrate that knock-down of Bcor results in
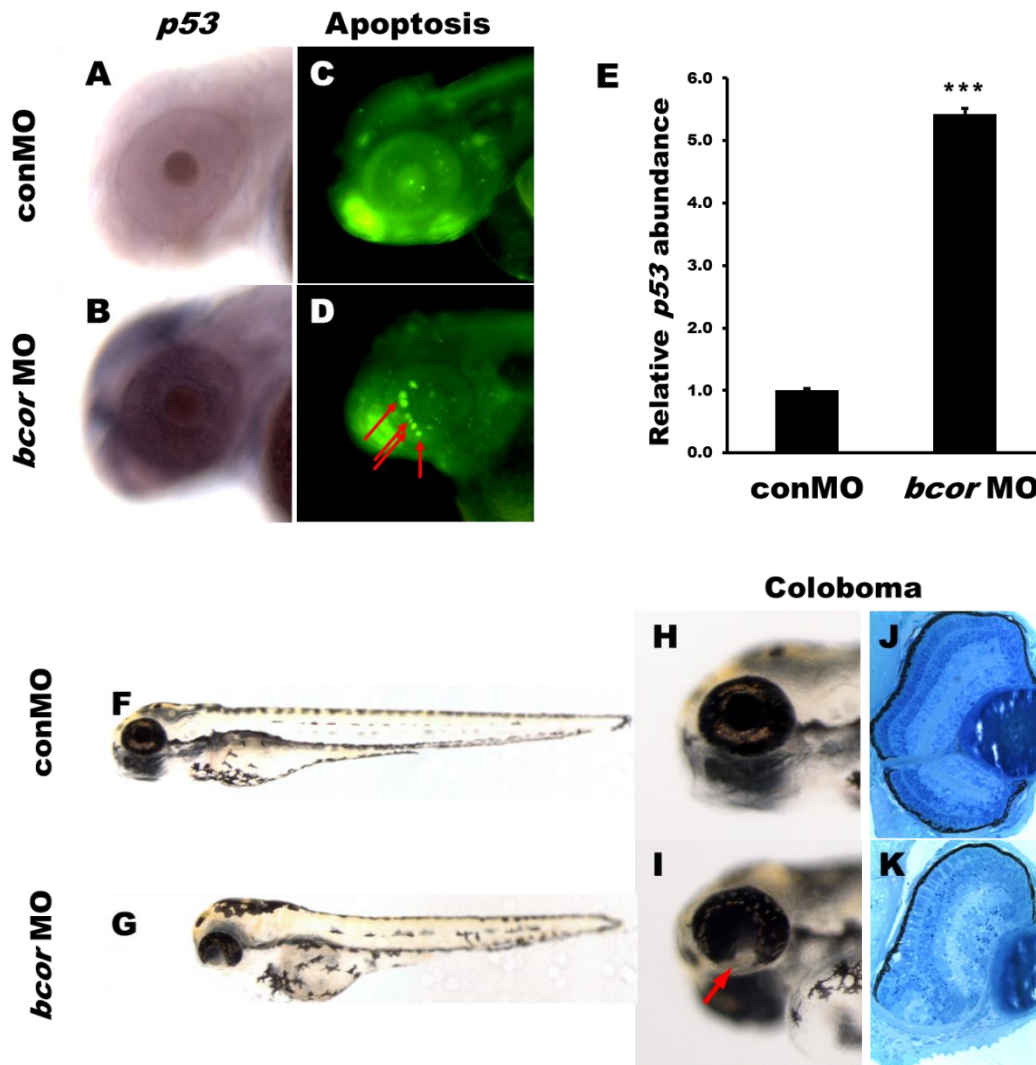
Figure III-10. Knock-down of Bcor results in the same phenotypes as knock-down of Bcl6.

p53 expression in (A) con-MO and (B) *bcor*-MO injected embryos at 48 hpf. *p53* expression domain is extended in the retina of Bcor deficient embryos. (E) Quantitative anaylsis by qRT-PCR shows a 5.4 fold increase of *p53* levels in *bcor*-MO injected embryos. Acridine orange staining in (D) con-MO and (E) *bcor*-MO injected embryos at 48 hpf. Bcl6 deficient embryos present with an increased number of apoptotic cells in the retina (arrows in panel D). (F-I) Knock-down of Bcor results in colobomas (arrows in panel I) and shortened bodies at 3 dpf. (J,K) Transverse histological sectioning of *bcor*-MO injected embryos at 3 dpf shows extrusion of retinal tissue and RPE.

62

the same molecular phenotypes as knock-down of Bcl6, suggesting that Bcor may work as a cofactor for Bcl6 in the developing eye.

Previous cell culture studies that utilized B cells demonstrated that Bcor co-immunoprecipitates with Bcl6 (Gearhart et al. 2006), suggesting that Bcor physically interacts with Bcl6. To investigate if Bcor functionally interacts with Bcl6 in the eye, I performed synergistic interaction analysis using injection of *bcl6*-MO and/or *bcor*-MO. To make sensitized conditions that do not lead to colobomas individually, I reduced the amount of *bcl6*-MO from 7.5ng to 1.5ng, and of *bcor*-MO from 1ng to 0.5ng, amounts that did not result in any observable phenotypes (Figs. III-11A-F). However, co-injection of 1.5ng *bcl6*-MO and 0.5ng *bcor*-MO resulted in colobomas and a shortened body in 68% of injected embryos (n=31) (Figs. III-11G,H), suggesting that Bcl6 and Bcor functionally interact in the eye.

III. 2. 7. Hdac1 and Bcl6 functionally interact in the eye.

Mutations in zebrafish *hdac1* result in colobomas (Yamaguchi et al., 2005; Stadler et al., 2005), and the transcriptional repressive function of Bcl6 requires histone deacetylase activity in cell culture (Bereshchenko et al., 2002). Thus, it is possible that Hdac1 is another co-factor required for Bcl6 to function in the eye. To test if a mutation in *hdac1* results in similar molecular phenotypes as *bcl6*-MO injected embryos, I performed *in situ* hybridization to examine *p53* expression and acridine orange staining to detect apoptotic cells as described above. Dramatic increase of *p53* expression was shown in *hdac1* homozygous mutant embryos at 48 hpf, while there was little expression

63

Figure III-11. Bcl6 and Bcor functionally interact in the eye.

(A,B) Wild-type embryos with normal activities of Bcl6 and Bcor develop normally. (C,D) Reducing the activity of Bcl6 by injecting low amounts of *bcl6*-MO (1.5ng) does not affect normal development. (E,F) Embryos injected with a low amount of *bcor*-MO (0.5ng) show normal development. (G,H) Co-injection of *bcl6*-MO (1.5ng) and *bcor*-MO (0.5ng) results in colobomas (arrow in panel H).

of *p53* in wild-type embryos (Figs. III-12A,B). qRT-PCR data revealed a 1.9 fold increase of *p53* expression in *hdac1* homozygous mutants compared to that in wild-type embryos ($p<0.0001$; t Test) (Fig. III-12C). *hdac1* mutants also presented with scattered apoptotic cells in the retina, while no apoptotic cells were detected in wild-type embryos at 48 hpf (Figs. III-12E,F). These data indicate that loss of Hdac1 function causes similar molecular phenotype to loss of Bcl6 function.

To investigate if Hdac1 functions with Bcl6, I performed a similar synergistic interaction analysis using *bcl6*-MO injection and Trichostatin-A (TSA) treatment. TSA is a chemical inhibitor of histone deacetylase activity and previous studies have shown that TSA treatment recapitulates the coloboma phenotype in *hdac1* homozygous mutants (Yamaguchi et al., 2005). I utilized sensitized conditions of Hdac1 activity which do not lead to any phenotypes (including colobomas) by reducing the concentration of TSA to 700nM and treating at a later time point (24 hpf). The embryos treated with TSA at this sub-optimal level developed normally (Figs III-13A-D). When I reduced the injection amount of *bcl6*-MO from 7.5ng to 2ng, the injected embryos didn't present with any detectable phenotypes (Figs. III-13E,F). However, when I treated 2ng *bcl6*-MO injected embryos with 700nM TSA from 24 hpf to 72 hpf, the embryos presented with colobomas and curved body (81%, n=27), similar to the *hdac1* and *bcl6*-MO phenotype (Figs. III-13G,H,H'). These results suggest that Hdac1 functionally interacts with Bcl6 in the eye.
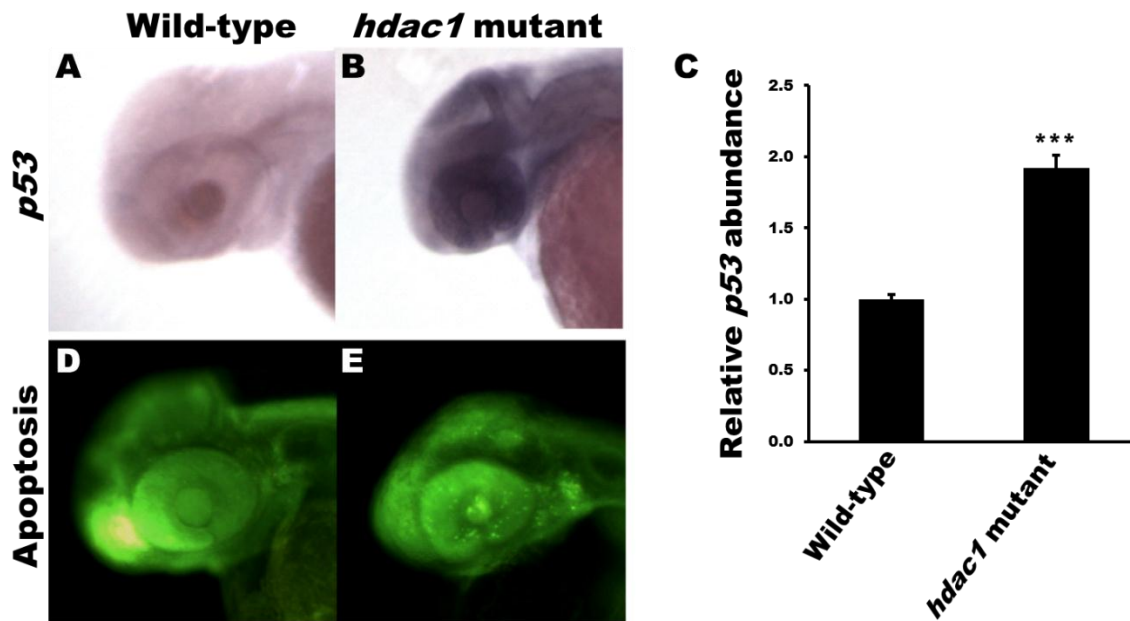
Figure III-12. Mutation in *hdac1* results in the same molecular phenotypes as knock-down of Bcl6.

p53 expression in (A) wild-type and (B) *hdac1* mutants embryos at 48 hpf. *p53* expression domain is extended in the retina of *hdac1* mutants. (C) Quantitative analysis by qRT-PCR shows a 1.9 fold increase of *p53* levels in *hdac1* mutants. Acridine orange staining in (D) wild-type and (E) *hdac1* mutants embryos at 48 hpf. *hdac1* mutants present with increased number of apoptotic cells in the retina.
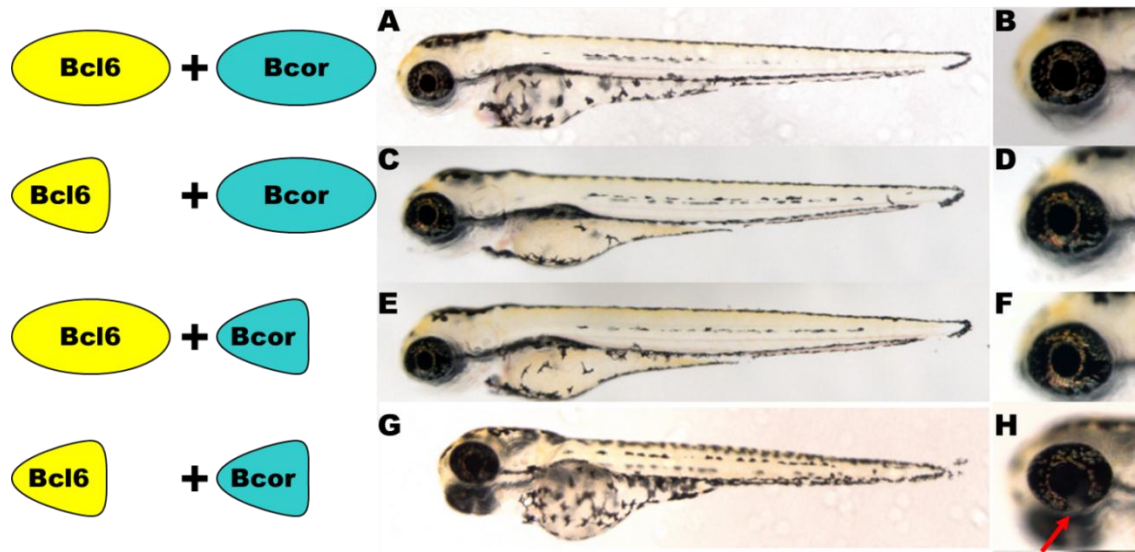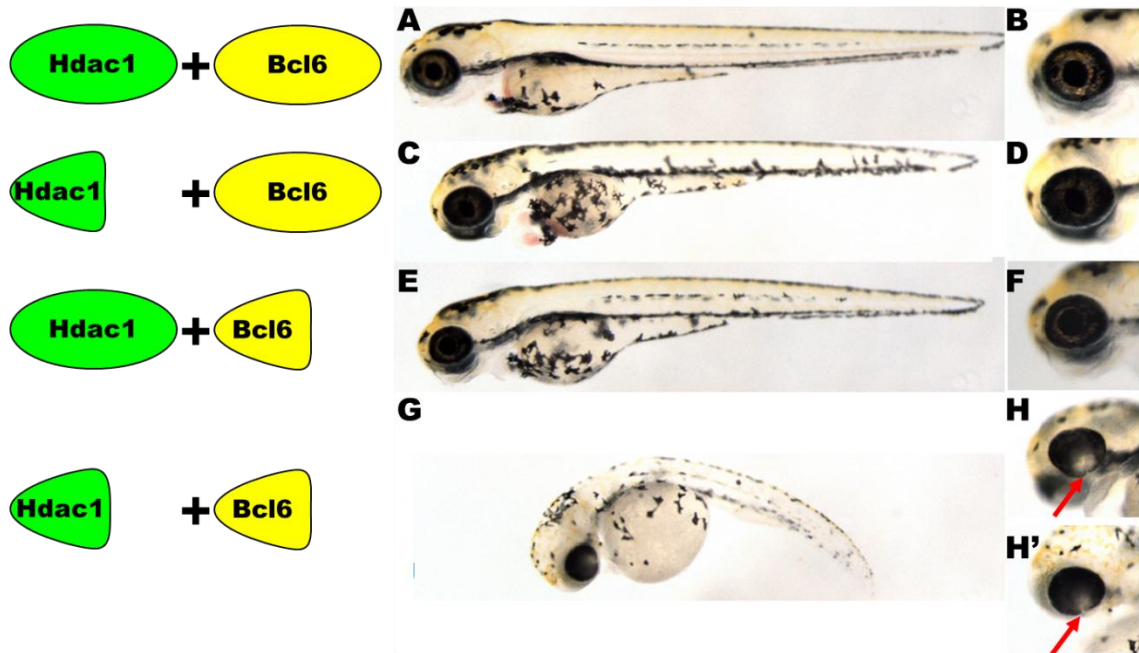
Figure III-13. Bcl6 and Hdac1 functionally interact in the eye.

(A,B) Wild-type embryos with full activities of Bcl6 and Hdac1 develop normally. (C,D) Embryos treated with a low concentration of TSA (700nM) show normal development. (E,F) Reduced activity of Bcl6 by injection of a low amount of *bcl6*-MO (1.5ng) does not affect normal development. (G,H,H') Treatment of TSA (700nM) into the embryos injected with *bcl6*-MO (1.5ng) results in colobomas (arrow in panel H) and curved bodies.

III. 2. 8. Bcor and Hdac1 functionally interact in the eye.

Since Bcor and Hdac1 are cofactors that functionally interact with Bcl6, it is plausible that Bcor and Hdac1 also functionally interact with each other. In cell culture, there was evidence that Bcor physically binds to Hdac1 (Huynh et al., 2000), supporting the possibility that they might works together in the eye. I performed a similar synergistic interaction analysis with *bcor*-MO injection and TSA treatment as previous interaction analyses. I utilized sensitized conditions of Hdac1 activity which do not lead to any phenotypes (including colobomas) by reducing the concentration of TSA to 500nM and treating at a later time point (24 hpf). The embryos treated with TSA at this sub-optimal level developed normally (Figs. III-14A-D). When I reduced the injection amount of *bcor*-MO from 1.0ng to 0.5ng, the injected embryos didn't present with any detectable phenotypes (Figs. III-14E,F). However, when I treated 0.5ng *bcor*-MO injected embryos with 500nM TSA from 24 hpf to 72 hpf, the embryos presented with colobmas and curved body as in *hdac1* homozygous mutants and 1.0ng *bcor*-MO injected embryos (86%, n=29) (Figs. III-14G,H,H').

To further confirm the functional interaction between Bcor and Hdac1, I performed a second interaction analysis by injecting 0.5ng of *bcor*-MO into *hdac1* heterozygous embryos. In the *hdac1* heterozygous embryos, loss of Hdac1 activity by half is not enough to cause developmental defects like coloboma, thus can be considered as another sensitized condition especially for Hdac1. As in the previous experiment, the wild-type embryos injected with 0.5ng of *bcor*-MO developed normally. But when I injected the same amount of *bcor*-MO into the pool of embryos drived from a cross of
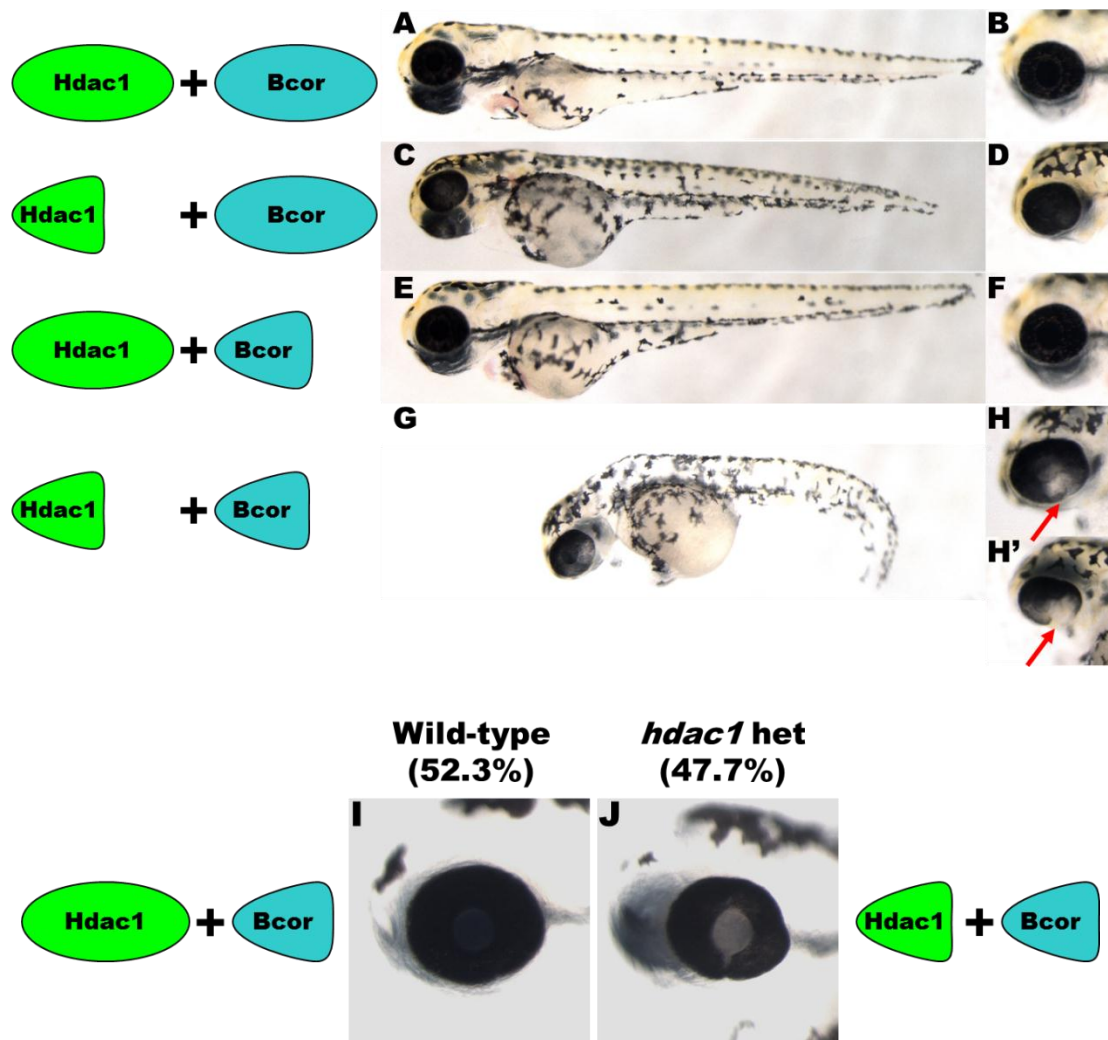
Figure III-14. Bcor and Hdac1 functionally interact in the eye.

(A,B) Wild-type embryos with full activities of Bcor and Hdac1 develop normally. (C,D) Embryos treated with a low concentration of TSA (500nM) show normal development. (E,F) Reduced activity of Bcor by injection of a low amount of *bcor*-MO (0.5ng) does not affect normal development. (G,H,H') TSA (500nM) Treatment of *bcor*-MO (0.5ng) injected embryos results in colobomas (arrow in panel H) and curved bodies. (I) Injection of *bcor*-MO (0.5ng) into wild-type siblings does not have any effect on normal development. (J) Injection of *bcor*-MO (0.5ng) into *hdac1* heterozygous siblings results in colobomas.

hdac1 heterozygote male and wild-type female, which were theoretically expected as the mixture of 50% heterozygotes and 50% wild-type siblings, 47.7% of the injected embryos showed colobomas in the eye and shortened body phenotypes (Figs. III-14I,J). In addition, genotyping of 5 embryos with colobomas confirmed that all of them were *hdac1* heterozygotes. These results support a model in which Hdac1 has a functional interaction with Bcor to regulate eye formation.

III. 3. DISCUSSION

In this study, I elucidated the function and regulation of Bcl6, a transcriptional repressor, in the developing zebrafish eye. Loss of Bcl6 function resulted in colobomas and ventral retina defects, demonstrating that Bcl6 plays a critical role in preventing apoptosis in the retina during eye development, and this is required to contain the retina and RPE within the optic cup. I also showed that Vax1 and Vax2 act upstream of *bcl6* in the ventral retina, and Bcl6 functions along with Bcor and Hdac1 to mediate cell survival by regulating *p53* within the developing zebrafish retina (Fig. III-15).

III. 3. 1. Knock-down of Bcl6 results in colobomas in developing zebrafish eyes.

Morpholino knock-down analysis performed in zebrafish embryos demonstrates that loss of Bcl6 function results in ocular colobomas with defects in trunk formation. Given that there was a report that the knock-down technology using MO injection has possibility to cause off-target effects, mainly neural cell death through p53 activation (Robu et al., 2007), I confirmed that colobomas in *bcl6*-MO injected embryos resulted from the specific effects of loss of Bcl6 function in several ways. First, *bcl6*-MO injected
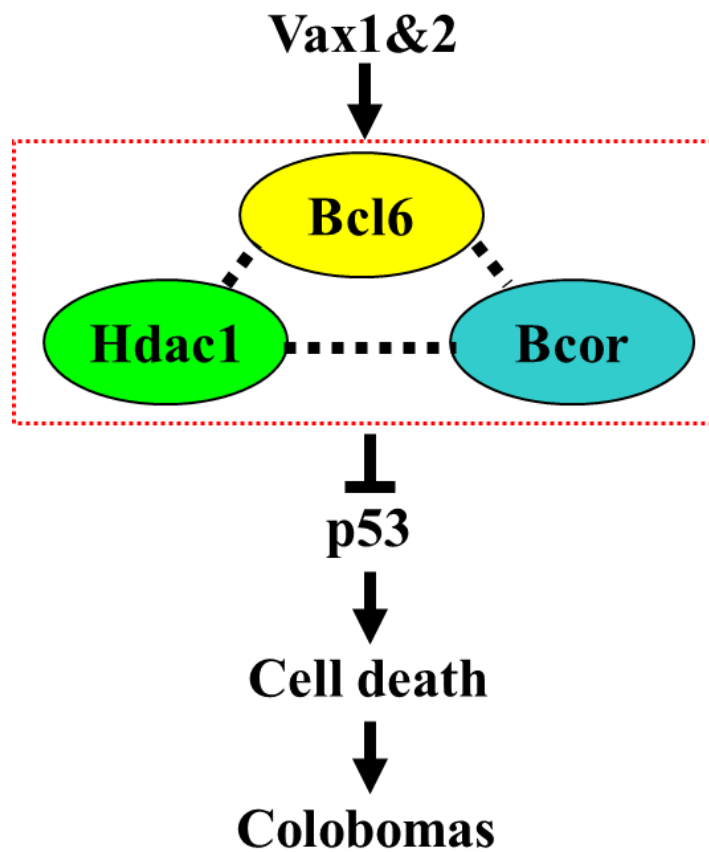
Figure III-15. Schematic diagram of the role of Bcl6 in CF closure.

embryos did not show smaller heads and eyes which usually result from neural cell death by off-target effects of MO. Histological analysis revealed that there was no disrupted retinal lamination and missing retinal cell types other than the colobomas. Secondly, a 5 base-pair mismatch MO designed within the *bcl6*-MO sequence did not have any effects on development at even higher injection amount than that of *bcl6*-MO. Thirdly, in addition to the splice blocking MO (*bcl6*-MO), I designed another MO (*bcl6*-MO2) that blocks translation of *bcl6* mRNA, and *bcl6*-MO2 injected embryos presented with similar phenotypes to *bcl6*-MO injected embryos. Since the neural death from non-specific effects is dependent on MO sequences (Robu et al., 2007), it is unlikely that two different MO sequences targeting the same gene would cause neural death; indeed, the similar results from two different MOs support that colobomas in the morphants are a specific phenotype resulting from loss of Bcl6 function. Furthermore, co-injection of *bcl6*-MO and *bcl6*-MO2 at sub-threshold levels resulted in colobomas. Moreover, knock-down of Bcl6 in another organism, *Xenopus*, phenocopied colobomas in Bcl6 knock-down zebrafish embryos. These results demonstrate that roles of Bcl6 in eye development are conserved between zebrafish and *Xenopus*, and that Bcl6 functions in preventing colobomas in the ventral retina. Finally, previous studies have shown that knock-down of Bcor, a co-repressor of Bcl6, results in a similar coloboma phenotype to Bcl6 knock-down in both zebrafish and *Xenopus* (Ng et al., 2004; Hilton et al., 2007), which further supports a model in which Bcl6 is required in the vertebrate eye for normal development.

III. 3. 2. Bcl6 is involved in regulating apoptosis in the eyes.

The function of BCL6 has been largely studied in B cells and is known to play a critical role in formation of germinal center and survival of B cells in germinal center (Dent et al., 1997). Given that the deregulation of Bcl6 from chromosomal rearrangement or point mutations in the 5' non-coding region is found in certain types of lymphomas (Ohno, 2004; Pasqualucci et al., 2003; Ye et al., 1995; Migliazza et al., 1995), regulation of BCL6 expression is deeply involved in controlling cell death and proliferation. In germinal center B cells, BCL6 inhibits *p53* expression induced by DNA damage caused by immunoglobulin class switching and somatic hypermutation, thus allowing B cells to survive (Phan and Dalla-Favera, 2004). In *bcl6*-MO injected embryos, *p53* expression is significantly increased along with increased cell death in the retina. Like in B cells, these results suggest that Bcl6 functions in the zebrafish retina to control apoptosis by suppressing *p53* expression. In many cell types that express Bcl6 (i.e. mammary epithelial cells and cells in the nervous system), terminal differentiation may be achieved by preventing apoptosis (Bajalica-Lagercrantz et al., 1998; Funatsu et al., 2004; Leamey et al., 2008; Logarajah et al., 2003; Otaki et al., 2005). Recently, it has been reported that BCL6 plays an important role in survival of differentiating olfactory sensory neurons (Otaki et al., 2010). Given that cells in the developing retina are in the process of differentiating, Bcl6 may work as an anti-apoptotic factor, allowing them enough time to differentiate. A previous study of apoptosis in the zebrafish retina showed that the number of apoptotic cells abruptly starts to increase after 30 hpf, peaks at 36 hpf, and drops dramatically before 48 hpf (Cole and Ross., 2001). My results make it plausible

that Bcl6 expressed in the retina may play an important role in controlling apopotosis by suppressing *p53* expression during this period.

III. 3. 3. Vax1 and Vax2 act upstream of *bcl6*.

In this study, I showed that loss of Vax1 and Vax2 resulted in a loss of *bcl6* expression, concomitant with induction of *p53*, and an increase in the number of apoptotic cells in the eye, suggesting that Vax1 and Vax2 act upstream of *bcl6* to regulate cell survival in the retina. Interestingly, co-knock-down of p53 along with Vax1/Vax2 rescued colobomas in *vax1/vax2* morphants, as in Bcl6 deficient embryos, providing further support that Vax1/Vax2 function upstream of *bcl6* during retina development. Previous studies in mouse lacking of Vax1 or Vax2 function revealed that defects in choroid fissure closure stemmed from a failure to restrict retinal cell fates to the optic cup (Barbieri et al., 2002; Bertuzzi et al., 1999; Hallonet et al., 1999; Mui et al., 2002). In zebrafish *vax1/vax2* morphants, a failure of choroid fissure closure was thought to result from cell fate changes in optic vesicle, causing an expansion of retina cell fates into optic nerve region (Take-uchi et al., 2003), which is a similar phenotype to that in the mouse knock-out. Here, I provided another possible mechanism by which Vax1/Vax2 may be required during eye development, which is in the control of apoptosis by regulating *bcl6* expression.

III. 3. 4. Bcl6 functionally interacts with Bcor and Hdac1.

Mutations in BCOR, a BCL6 corepressor, are known to be responsible for OFCD syndrome whose defects include ocular disease like microphthalmia and colobomas (Ng

et al., 2004; Gorlin et al., 1996; Schulze et al., 1999; Hedera and Gorski, 2003). Loss of function studies using knock-down of zebrafish Bcor recapitulated human OFCD syndrome with colobomas (Ng et al., 2004). Evidence from cell culture studies demonstrate that Bcl6 interacts with Bcor through its POZ/BTB domain and recruits Bcor with other corepressors to Bcl6 target genes like *p53* and *cyclin D2* (Gearheart et al., 2006). Left-right asymmetry patterning studies in *Xenopus* provided *in vivo* evidence supporting the possibility that Bcl6 functionally interacts with Bcor (Hilton et al., 2007; Sakano et al., 2010). Loss of function studies using MO knock-down technology for both Bcl6 and Bcor in *Xenopus* showed similar laterality defects like reversion of cardiac orientation and disorganized gut patterning as well as a similar molecular phenotype of down-regulation of *Pitx2* expression. My results from synergistic interaction analysis of Bcl6 and Bcor provided further *in vivo* evidence that Bcl6 and Bcor are functionally associated with each other, and this is required for normal eye development. Interestingly, colobomas resulting from either Bcl6 or Bcor knock-down in *Xenopus* resemble each other, suggesting that functional interaction of Bcl6 and Bcor plays an important role in the eye development of *Xenopus* as well.

Histone deacetylases (HDACs) are known to be involved in silencing transcription through epigenetic modification of histones, maintaining a transcriptionally inactive chromatin state (Sterner and Berger, 2000), or through directly regulating activity of transcription activators with controlling their cytosol/nuclear localization, affinities with co-factors, or abilities to bind DNA (Barlev et al., 2001). It has been reported that acetylation of BCL6 by p300 inactivate its function as a transcription

repressor and prevents recruiting co-factor complex including HDACs (Bereshchenko et al., 2002). Furthermore, studies using zebrafish *hdac1* homozygous mutants revealed that Hdac1 plays an important role in cell cycle exit and differentiation in the retina, and that loss of Hdac1 function results in severe colobomas (Stadler et al., 2005; Yamajuchi et al., 2005). In the developing mouse retina, HDAC activity is involved in regulating expression of the pro-apoptotic factors like Apaf-1 and Caspase3 in order to prevent apoptosis (Wallace and Cotter, 2008; Wallace et al., 2006). My results showed that *hdac1* homozygous mutants present with similar phenotypes to bcl6 deficient embryos, showing up-regulation of *p53* expression and increased number of apoptotic cells in the retina. These data suggest that BCL6 and HDACs might functionally interact with each other in the eyes. My synergistic interaction analysis showed that reduced activities of both Bcl6 and Hdac results in colobomas, while reduction of each of these alone did not affect eye development, demonstrating that Bcl6 functionally interacts with Hdac in the developing eye.

In addition, synergistic interaction analysis for Bcor and Hdac1 revealed that Bcor and Hdac1 are also functionally associated in the eye. Previous co-immunoprecipitation studies revealed that Hdac physically interact with Bcor (Huynh et al., 2000), supporting the cooperation of Bcor and Hdac1in the eye demonstrated here through functional analysis.

76

III. 3. 5. Possible molecular mechanisms by which Bcl6 functions during eye development.

Although the function, the target genes, and corepressors of Bcl6 have been studied in various contexts, the molecular mechanisms by which Bcl6 suppresses transcription remain to be elucidated. Intensive co-immunoprecipitation studies on associating partners for Bcl6 in cell culture systems provided a couple of possible mechanisms regulating transcription of target genes. It has been reported that a transcriptional repression complex, called the BCOR complex, includes FBXL10 and Polycomb group proteins, which are known to suppress transcription through epigenetic modification of chromatin, and that this complex is recruited by BCL6 to target genes (Gearheart et al., 2006). Furthermore, one of the Polycomb group components, RNF2, possesses E3 ligase activity and could mono-ubiquitinate H2A. Since mono-ubiquitylated H2A is considered to maintain a repressed state of chromatin, Bcl6 in recruiting the BCOR complex to target gene promoters, may recruit RNF2 in order to suppress transcription; indeed, enriched mono-ubiquitylated H2A was found at BCL6 target genes (*Cyclin D2* and *p53*) in B cells (Gearheart et al., 2006). Demethylation of H3 K36 through FBXL10, another BCOR complex member, is another possible mechanism underlying Bcl6-dependent repression. Methylation of H3 K36 is considered to promote transcription and FBXL10 possesses a JmjC demethylase domain, which is expected to specifically demethylate di-methylated H3 K36 (Tsukada et al., 2006; Bannister et al., 2005; Rao et al., 2005), suggesting FBXL10 may function to epigenetically repress transcription. Given that FBXL10 can be recruited as a component of Bcor complex to

Bcl6 target genes, Bcl6 may utilize the demethylase activity of FBXL10 to suppress transcription. Since BCOR associates with HDACs in mammalian cell culture (Huynh et al., 2000), Bcl6 can also bring Hdacs to target genes. Loss of Hdacl function in zebrafish embryos showed highly increased acetylation of histone H4 as well as apoptotic cells, resulting in colobomas (Stadler et al., 2005). And I showed that Bcor interacts genetically with Hdac1 in zebrafish. Thus, it is also plausible that the deacetylation of histones through Hdac1 may repress transcription of Bcl6 target genes. Future work will test these models and determine the mechanisms underlying Bcl6/Bcor function in regulating cell survival in the zebrafish eye.

CHAPTER IV

SUMMARY AND CONCLUSION

During optic cup morphogenesis, the neuroectodermal layers of the OV invaginate ventrally, and fuse at the choroid fissure along the proximo-distal axis such that the retina and RPE are confined within the cup. Failure of the choroid fissure to properly close during early eye development causes ocular malformations called colobomas, which are characterized by the persistence of a cleft or hole at the back of the eye, resulting in blindness. While choroid fissure closure is a critical aspect of ocular development, the molecular and cellular mechanisms underlying this process are poorly understood. During my Ph.D. research, I have focused on addressing molecular mechanisms underlying choroid fissure closure and colobomas.

In the first of my studies, I determined that early cell fate changes within the eye field could be responsible for choroid fissure closure defects that lead to colobomas (Lee et al., 2008). In this study I have characterized the ocular defects in the recessive zebrafish mutant *blowout* that presents with a variably penetrant coloboma phenotype. *blowout* mutants develop unilateral or bilateral colobomas and as a result, the retina and retinal pigmented epithelium are not contained within the optic cup. Colobomas result from defects in optic stalk morphogenesis whereby the optic stalk extends into the retina and impedes the lateral edges of the choroid fissure from meeting and fusing. The expression domain of the proximal optic vesicle marker *pax2a* is expanded in *blowout* at the expense of the distal optic vesicle marker *pax6*, suggesting that the initial patterning

79

of the optic vesicle into proximal and distal territories is disrupted in *blowout*. Later aspects of distal optic cup formation (i.e. retina development) are normal in *blowout* mutants, however. Positional cloning of *blowout* identified a nonsense mutation in *patched1*, a negative regulator of the Hedgehog pathway, as the underlying cause of the *blowout* phenotype. Expanded domains of expression of the Hedgehog target genes *patched1* and *patched2* were observed in *blowout*, consistent with a loss of Patched1 function and upregulation of Hedgehog pathway activity. Moreover, colobomas in *blowout* could be suppressed by pharmacologically inhibiting the Hedgehog pathway with cyclopamine, and maximal rescue occurred when embryos were exposed to cyclopamine between 5.5 and 13 hours post fertilization. These observations highlight the critical role that Hedgehog pathway activity plays in mediating patterning of the proximal/distal axis of the optic vesicle during the early phases of eye development and they provide genetic confirmation for the integral role that *patched1*-mediated negative regulation of Hedgehog signaling plays during vertebrate eye development.

In the second of my studies, I examined Bcl6 function and regulation during vertebrate eye development. *bcl6* encodes a transcriptional repressor expressed in the ventral retina during zebrafish eye development. Human BCL6 is involved in cell survival and cell cycle regulation in germinal center B cells, however, roles for Bcl6 in the eye have not been identified. Loss of Bcl6 function leads to colobomas and ventral retina defects. The role for Bcl6 in the eye is also conserved in *Xenopus*. *bcl6* knockdown also results in up-regulation of *p53*, a previously known Bcl6 target, and an increase in the number of apoptotic cells in the retina. Knockdown of both *bcl6* and *p53* prevents

80

colobomas supporting a model in which Bcl6 dependent *p53* inhibition in the retina is required for cell survival therein. These results demonstrate that Bcl6 plays a critical role in preventing apoptosis in the retina during eye development, and this is required to contain the retina and RPE within the optic cup. Loss of Vax1 and Vax2 in zebrafish leads to colobomas (Take-uchi et al., 2003), and I tested whether Vax1 and Vax2 act upstream of *bcl6*. Indeed, loss of Vax1 and Vax2 resulted in a loss of *bcl6* expression, concomitant with induction of *p53*, and an increase in the number of apoptotic cells in the eye. Interestingly, triple knockdown of *vax1*, *vax2* and *p53* rescued colobomas in *vax1/vax2* morphants suggesting that Vax1 and Vax2 act upstream of *bcl6* to regulate cell survival in the retina. Finally, I identified functional interactions between Bcl6, Bcor and Hdac1 during eye development, suggesting that Bcl6 functions along with Bcor and Hdac1 to mediate cell survival by regulating *p53* within the developing zebrafish retina.

Combined, my studies expand the gene regulatory network involved in cell fate determination and cell survival during CF closure and ventral retina formation, and provide mechanistic insight into coloboma formation (Fig. IV-1) and they will further our ability to identify and develop possible therapies for colobomas, enabling the patients to retain some of their vision.
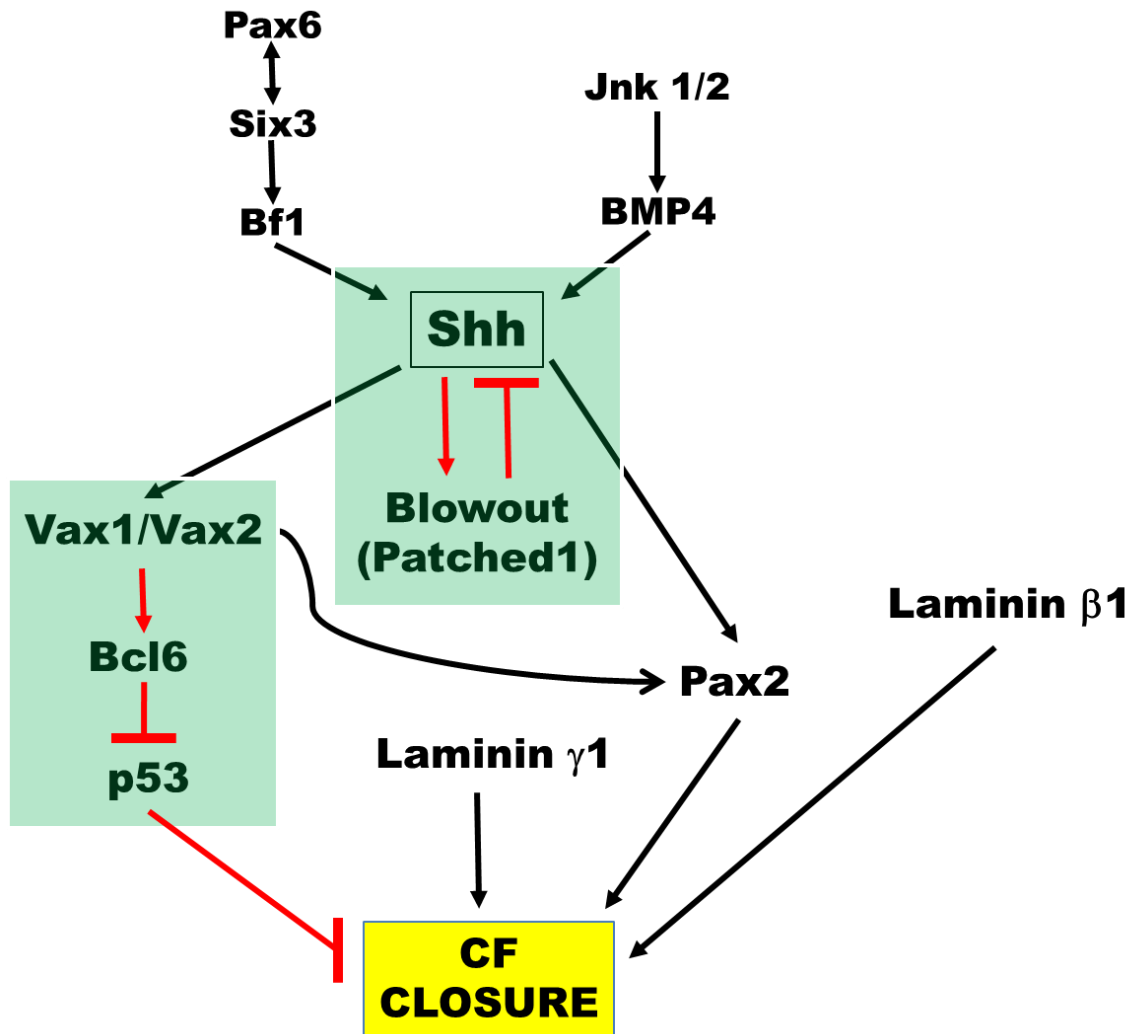
Figure IV-1. Gene regulatory network underlying ventral retina formation and choroid fissure closure.

In this schematic diagram, my research findings are highlighted by red lines and light blue backgrounds.

Appendix A : Materials and Methods

A.1. ZEBRAFISH MAINTENANCE AND STRAINS

Zebrafish (*Danio rerio*) were maintained at 28.5°C on a 14h light/10h dark cycle. Embryos were obtained from the natural spawning of heterozygous carriers or homozygous mutants setup in pairwise crosses. Embryos were collected and raised at 28.5°C after Westerfield (1995) and were staged according to Kimmel et al. (1995). *blw*^{tc294z} outcrosses were provided by Dr. Hans Georg Frohnhöfer at the Max Planck Institute for Developmental Biology and were propagated by repeated outcrosses to TL fish. *hdac1*^{hi1618Tg} outcrosses were provided by Zebrafish International Resource Center (ZIRC) at the University of Oregon and were propagated by repeated outcrosses to AB fish. All animals were treated in accordance with provisions established at the University of Texas at Austin governing animal use and care.

A.2. HISTOLOGY

Histology was performed as described in Nuckels and Gross (2007). Briefly, embryos were collected and fixed overnight at 4°C in a solution of 1% (w/v) paraformaldehyde (PFA), 2.5% glutaraldehyde and 3% sucrose in phosphate buffered saline (PBS). They were washed 3 × 5 minutes (min) in PBS and re-fixed for 90 min at 4°C in a 2% OsO$_4$ solution, washed 3 × 5 min in PBS at room temperature (RT) and dehydrated through a graded ethanol series (50, 70, 80, 90, 2 × 100%). Embryos were further dehydrated 2 × 10 min in propylene oxide and infiltrated 1–2 hours in a 50%

propylene oxide/50% Epon/Araldite mixture (Polysciences, Inc.). Embryos were then incubated overnight at RT in 100% Epon/Araldite resin with caps open to allow for propylene oxide evaporation and resin infiltration, embedded and baked at 60°C for 2–3 days. Sections 1–1.25 um were cut, mounted on glass slides and stained in a 1% methylene blue/1% borax solution. Sections were mounted in DPX (Electron Microscopy Sciences) and photographed on a Leica DMRB microscope mounted with a DFC320 digital camera.

A.3. IMMUNOHISTOCHEMISTRY

Laminin immunohistochemistry was performed as described in Lee and Gross (2007). Briefly, embryos were collected and fixed overnight at 4°C in a solution of 4% PFA and 3% sucrose in PBS. Embryos were washed at RT 3 × 5 min in PBS and processed immediately for whole mount immunohistochemistry. Whole-mount embryos were washed in PBS/0.1% TIen-20 (PBST) and permeabilized 12' with 100% acetone prechilled to −20°C. Embryos were washed three times at RT with PBST and digested with proteinase K (10ug/mL diluted in PBST) for 12–30 minutes depending on age. Embryos were then washed with PBST, refixed in 4% PFA for 10' at RT, washed 3x in PBST and blocked for 1 hour at RT in block [2% normal goat serum (NGS), 1% DMSO in PBST]. Embryos were then incubated overnight at 4°C in anti-laminin-111 antibody (Sigma) diluted 1:400 in block. Embryos were washed 5x 30' in PBST and incubated overnight at 4°C in biotin-SP conjugated affinity purified F(ab')$_2$ goat anti-rabbit IgG diluted 1:500 in block. Embryos were then washed 5x 30' in PBST and incubated 3 hours

at RT in Avidin-Peroxidase Complex Reagent (ABC Reagent; Vector Labs). Embryos were washed 3x 30' in PBST and then developed for 10–30' with DAB reagent (Sigma). After development, embryos were fixed briefly in 4%PFA, cryosectioned and imaged as above. Immunohistochemistry with zpr1, zpr3 and zn8 monoclonal antibodies (Zebrafish International Resource Center) was performed as described in Uribe and Gross (2007). Primary antibodies were diluted at 1:200, Cy3 secondary antibody at 1:300 and Sytox-Green (Molecular Probes) at 1:10,000. Imaging was performed on a Zeiss LSM5 Pascal laser scanning confocal microscope. 3–5 optical sections (1um in thickness) were collected and projected using Zeiss confocal software. Images were overlaid using Adobe Photoshop CS2.

A.4. 5-BROMO-2-DEOXYURIDINE (BRDU) STAINING

Embryos were dechorionated and incubated in fish water with 10mM BrdU (Sigma) for defined time periods and either immediately sacrificed or washed three times into fish water and grown for additional periods before sacrifice. Embryos were processed for immunohistochemistry after Uribe and Gross (2007) with the addition of a 10 min incubation in 4N HCl at 37° prior to blocking to relax chromatin and facilitate BrdU detection. Mouse anti-BrdU was used at a 1:50 dilution and Cy3 anti-mouse secondaries were used at a 1:200 dilution. Nuclei were counterstained with Sytox-Green (1:10,000; Molecular Probes). Imaging was performed on a Zeiss LSM5 Pascal laser scanning confocal microscope. 3–5 optical sections (1um in thickness) were collected and projected using Zeiss confocal software. BrdU positive cells and nuclei were counted in

three to five eyes from different embryos and averages were compared by Fisher's exact test for statistical significance (Graphpad Prism).

A.5. POSITIONAL CLONING

Mapping was essentially performed as in (Willer et al., 2005). A mapping panel was generated by outcrossing a TL+/*blw* with a WIK +/+ fish and then backcrossing a resulting WIK+/*blw* male with a TL+/*blw* female. Genomic DNA was isolated from homozygous embryos and wild-type siblings and used for bulk segregant analysis. Simple sequence length polymorphisms (SSLPs) roughly 20cM apart across the genome were amplified by PCR and analyzed on E-Gel 4% agarose gels (Invitrogen). Once linkage was detected, 96 individual mutants were genotyped to confirm linkage and refine the interval. For high-resolution mapping, new mapping panels were created by backcrossing two individual WIK+/*blw* females to TL+/*blw* males to create homozygous mutants. Flanking markers Z11410 and Z13521 were used to genotype a total of 526 mutant embryos. The Ensembl Zv6 Zebrafish assembly was used to identify completed BAC sequences in the interval and new markers were designed within these BACs using the Zebrafish SSR search website (http://danio.mgh.harvard.edu/markers/ssr.html). A 917kb critical interval was identified and the open reading frames (ORFs) from six candidate loci in the interval were cloned and sequenced from *blw* and wild-type embryos using Big-Dye chemistry and an ABI 3130XL DNA sequencer (Applied Biosystems). Mutations in *atp6v0b* (NM_199561) and *ptc1* (NM_130988) were identified. A *ptc1* mutation in *blw* was first reported by Koudijs et al., (2008). Confirmation of the

identified T→A mutation at position 520 in *atp6v0b* was obtained by genotyping genomic DNA from mutant, WIK+/*blw*, and TL+/*blw* fish using a SNP assay run on a PSQ HS 96 Pyrosequencer (Biotage AB). Confirmation of the identified G→A mutation at position 3119 in *ptc1* was obtained by PCR amplifying the corresponding region of genomic DNA from mutant, WIK+/*blw* and TL+/*blw* fish and then direct sequencing. G3119A also disrupts a conserved AvaII restriction site enabling *blw* mutants to be genotyped by restriction fragment length polymorphism (RFLP) assays where genomic DNA was isolated from embryos and a region of the *ptc1* gene from Exon 16 (5' - CCA TGA TAA GTA CGA CAC CAC TGG AGA G - 3') to Intron 17 (5' - CAC TAC ACC AAA TCC CTG ATG GAT GG - 3') spanning the mutation was PCR amplified, gel purified, digested overnight with AvaII and analyzed on a 2% agarose gel.

A.6. MORPHOLINO, mRNA AND BAC INJECTIONS

ptc1, atp6v0b, vax1, and *vax2* morpholinos (MOs) were purchased from Open Biosystems (Huntsville, AL). *bcl6*-MO*, bcl6*-MMO*, bcor*-MO*,* and *p53*-MO were purchased from Gene Tools (Philomath, OR). MOs were resuspended in water and injections performed at the 1-cell stage into wild-type Oregon AB embryos. A standard control morpholino (5'-CCTCTTACCTCAGTTACAATTTATA-3') was used for injection control embryos and 13ng was injected. *Ptc1*MO (5'-CATAGTCCAAACGGGAGGCAGAAGA-3') targeted the translation initiation site of the *ptc1* transcript (Wolff et al., 2003) and 1.3 ng was injected into 1-cell stage wild-type Oregon AB embryos. *atp6v0b* MO (5'-AAGGTTTTATTAGCACTTACCGACG-3')

targeted the exon1/intron1 junction of the *atp6v0b* transcript and 13 ng was injected into 1-cell stage wild-type Oregon AB embryos. Splicing was verified by RT-PCR as described in (Gross and Dowling, 2005). *Bcl6*-MO (5′-GCAAGCAGCCTTCAATTGTACCTGC-3') targeted the exon2/intron2 junction of the *bcl6* transcript and 7.5 ng was injected into 1-cell stage wild-type Oregon AB embryos. *bcor*-MO (Ng et al., 2004) targeted the exon12/intron12 junction of the *bcor* transcript and 1.0 ng was injected into 1-cell stage wild-type Oregon AB embryos. *vax1*-MO (3.7ng) and *vax2*-MO (3.7ng) (Take-uchi et al., 2003) was injected into 1-cell stage wild-type Oregon AB embryos. For mRNA overexpression, full-length *ptc1* was PCR amplified and subcloned into pCR4-TOPO, and *atp6v0b* and *atp6v0b*^{N113K} were PCR amplified and subcloned into pCS2. Plasmid containing cDNAs were linearized and used for *in vitro* translation (mMessage Machine, Ambion). mRNA was resuspended in water and 50 and 100pg was injected into embryos derived from $blw^{+/-} \times blw^{+/-}$, $blw^{-/-} \times blw^{+/-}$ crosses and/or 1-cell stage wild-type Oregon AB embryos. BAC DKEY-31M5 was purchased from RZPD (Berlin, Germany), isolated from bacteria (Qiagen) and injected into 1-cell stage embryos derived from heterozygous *blw* incrosses.

A.7. RIBOPROBES AND *IN SITU* HYBRIDIZATION

Hybridizations were performed essentially as described by JoItt and Lettice using digoxigenin labeled antisense RNA probes (JoItt and Lettice, 1994). *ptc1 and p53* was cloned from 24hpf cDNA, ligated into pGEM-T and used for probe synthesis (cloning details available upon request). *In situ* hybridizations on embryos younger than 48hpf

was performed on embryos derived from homozygous incrosses such that all embryos were mutant and genotyping was unnecessary. Probe synthesis constructs for the listed genes were generously provided by the following researchers: *pax2a* (Bruce Riley, Texas A+M University), *ptc2* (Brian Perkins, Texas A+M University), *pax6* (Brian Link, Medical College of Wisconsin), and *bcl6* (Zebrafish International Resource Center).

A.8. CYCLOPAMINE AND TRICHOSTATIN A (TSA) TREATMENTS

Cyclopamine (Sigma) was resuspended at 10mg/mL in 100% ethanol and diluted into fish water for exposures. 100% ethanol was used for vehicle controls. Embryos derived from homozygous *blw* incrosses were used for all exposures. Embryos were removed from cyclopamine at defined times and washed into fish water for further culturing. Cyclopamine rescue data was analyzed by Fisher's exact test for statistical significance (Graphpad Prism).

TSA stock solution (Sigma, 1 mg/ml in DMSO) was diluted to appropriate concentrations for use. Embryos were incubated in TSA-containing fish water from 24 hpf to 72 hpf and immediately fixed with 4% PFA.

A.9. PREPARATION OF *XENOPUS* EMBRYOS AND MORPHOLINO INJECTION

Xenopus laevis embryos were de-jellied using a 3% cysteine solution in 1/3X MMR. Anti-sense morpholino oligonucleotides for Bcl6 (Sakano et al., 2010) was injected into one of dorsal cells at the 4 cell stage and were incubated until proper developmental stage (Nieuwkoop and Faber, 1994). The injected embryos were fixed at

stage 41 with 1X MEMFA (0.1 M MOPS, 2 mM EGTA, 1 mM MgSO4, 3.7% formaldehyde, pH 7.4).

A.10. QUANTITATIVE REAL-TIME RT-PCR (QRT-PCR)

Total RNA was also extracted from con-MO injected, *bcl6*-MO injected, *bcor*-MO injected, or *vax1/vax2* MO injected, or *hdac1* homozygous mutants embryos at 48 hpf using TRIzol reagent (Invitrogen). The total RNA was reverse-transcribed using iScript^{TM} cDNA Synthesis Kit (BIO-RAD). Relative gene expression levels were quantified using Power SYBR Green dye (Applied Biosystems) and an ABI PRISM 7900HT real-time PCR cycler (ABI SDS 2.3 software). All samples were analyzed in triplicate and relative transcript abundance was normalized to expression of *β-actin* using the 2 (-delta delta C(T)) method (Livak and Schmittgen, 2001). Primers used to assay gene expression were designed across exon boundaries of *p53*. Primers were as follows: *p53* forward 5'-CCC ATC CTC ACA ATC ATC ACT CTG G-3', reverse 5'-TCT CCT CAG TTT TCC TGT CTC TGC C-3'; *β-actin* forward 5'- CCA AAG CCA ACA GAG AGA AGA TGA C-3', reverse 5'- TAC AGA GAG AGC ACA GCC TGG ATG -3';

A.11. ACRIDINE ORANGE STAINING

Embryos were incubated for 30 min in fish water with 5 μg/ml acridine orange (Sigma). The embryos were washed three times for 5 min in fish water. The embryos were then anaesthetized and Fluorescence signal was detecteded immediately under a fluorescence microscope using a rhodamine filter set.

References

Adler, R., Canto-Soler, M. V., 2007. Molecular mechanisms of optic vesicle development: complexities, ambiguities and controversies. Dev Biol. 305**,** 1-13.

Adolphe, C., et al., 2006. Patched1 functions as a gatekeeper by promoting cell cycle progression. Cancer Res. 66**,** 2081-8.

Agathocleous, M., et al., 2007. A general role of hedgehog in the regulation of proliferation. Cell Cycle. 6**,** 156-9.

Allman, D., et al., 1996. BCL-6 expression during B-cell activation. Blood. 87**,** 5257-68.

Amato, M. A., et al., 2004. Hedgehog signaling in vertebrate eye development: a growing puzzle. Cell Mol Life Sci. 61**,** 899-910.

Amsterdam, A., et al., 2004. Identification of 315 genes essential for early zebrafish development. Proc Natl Acad Sci U S A. 101**,** 12792-7.

Bajalica-Lagercrantz, S., et al., 1998. Expression of the BCL6 gene in the pre- and postnatal mouse. Biochem Biophys Res Commun. 247**,** 357-60.

Bannister, A. J., et al., 2005. Spatial distribution of di- and tri-methyl lysine 36 of histone H3 at active genes. J Biol Chem. 280**,** 17732-6.

Barbieri, A. M., et al., 2002. Vax2 inactivation in mouse determines alteration of the eye dorsal-ventral axis, misrouting of the optic fibres and eye coloboma. Development. 129**,** 805-13.

Barbieri, A. M., et al., 1999. A homeobox gene, vax2, controls the patterning of the eye dorsoventral axis. Proc Natl Acad Sci U S A. 96**,** 10729-34.

Bardwell, V. J., Treisman, R., 1994. The POZ domain: a conserved protein-protein interaction motif. Genes Dev. 8**,** 1664-77.

Barlev, N. A., et al., 2001. Acetylation of p53 activates transcription through recruitment of coactivators/histone acetyltransferases. Mol Cell. 8**,** 1243-54.

Baron, B. W., et al., 1993. Identification of the gene associated with the recurring chromosomal translocations t(3;14)(q27;q32) and t(3;22)(q27;q11) in B-cell lymphomas. Proc Natl Acad Sci U S A. 90**,** 5262-6.

Barresi, M. J., et al., 2000. The zebrafish slow-muscle-omitted gene product is required for Hedgehog signal transduction and the development of slow muscle identity. Development. 127**,** 2189-99.

Barth, K. A., Wilson, S. W., 1995. Expression of zebrafish nk2.2 is influenced by sonic hedgehog/vertebrate hedgehog-1 and demarcates a zone of neuronal differentiation in the embryonic forebrain. Development. 121**,** 1755-68.

Beales, P. L., et al., 2007. IFT80, which encodes a conserved intraflagellar transport protein, is mutated in Jeune asphyxiating thoracic dystrophy. Nat Genet. 39**,** 727-9.

Bereshchenko, O. R., et al., 2002. Acetylation inactivates the transcriptional repressor BCL6. Nat Genet. 32**,** 606-13.

Bermejo, E., Martinez-Frias, M. L., 1998. Congenital eye malformations: clinical-epidemiological analysis of 1,124,654 consecutive births in Spain. Am J Med Genet. 75, 497-504.

Bertuzzi, S., et al., 1999. The homeodomain protein vax1 is required for axon guidance and major tract formation in the developing forebrain. Genes Dev. 13, 3092-105.

Black, G. C., et al., 2003. Abnormalities of the vitreoretinal interface caused by dysregulated Hedgehog signaling during retinal development. Hum Mol Genet. 12, 3269-76.

Cao, R., et al., 2005. Role of Bmi-1 and Ring1A in H2A ubiquitylation and Hox gene silencing. Mol Cell. 20, 845-54.

Cattoretti, G., et al., 1995. BCL-6 protein is expressed in germinal-center B cells. Blood. 86, 45-53.

Chang, C. C., et al., 1996. BCL-6, a POZ/zinc-finger protein, is a sequence-specific transcriptional repressor. Proc Natl Acad Sci U S A. 93, 6947-52.

Chang, L., et al., 2006. Uveal coloboma: clinical and basic science update. Curr Opin Ophthalmol. 17, 447-70.

Chen, Y., Struhl, G., 1996. Dual roles for patched in sequestering and transducing Hedgehog. Cell. 87, 553-63.

Chiang, C., et al., 1996. Cyclopia and defective axial patterning in mice lacking Sonic hedgehog gene function. Nature. 383, 407-13.

Chow, R. L., Lang, R. A., 2001. Early eye development in vertebrates. Annu Rev Cell Dev Biol. 17, 255-96.

Cole, L. K., Ross, L. S., 2001. Apoptosis in the developing zebrafish embryo. Dev Biol. 240, 123-42.

Concordet, J. P., et al., 1996. Spatial regulation of a zebrafish patched homologue reflects the roles of sonic hedgehog and protein kinase A in neural tube and somite patterning. Development. 122, 2835-46.

Cooper, M. K., et al., 1998. Teratogen-mediated inhibition of target tissue response to Shh signaling. Science. 280, 1603-7.

Dakubo, G. D., et al., 2003. Retinal ganglion cell-derived sonic hedgehog signaling is required for optic disc and stalk neuroepithelial cell development. Development. 130, 2967-80.

De Jong, P. T., et al., 1985. Medullated nerve fibers. A sign of multiple basal cell nevi (Gorlin's) syndrome. Arch Ophthalmol. 103, 1833-6.

de Napoles, M., et al., 2004. Polycomb group proteins Ring1A/B link ubiquitylation of histone H2A to heritable gene silencing and X inactivation. Dev Cell. 7, 663-76.

Dent, A. L., et al., 1997. Control of inflammation, cytokine expression, and germinal center formation by BCL-6. Science. 276, 589-92.

Dhordain, P., et al., 1997. Corepressor SMRT binds the BTB/POZ repressing domain of the LAZ3/BCL6 oncoprotein. Proc Natl Acad Sci U S A. 94, 10762-7.

Dhordain, P., et al., 1998. The LAZ3(BCL-6) oncoprotein recruits a SMRT/mSIN3A/histone deacetylase containing complex to mediate transcriptional repression. Nucleic Acids Res. 26, 4645-51.

Dutta, S., et al., 2005. pitx3 defines an equivalence domain for lens and anterior pituitary placode. Development. 132, 1579-90.

Ekker, S. C., et al., 1995. Patterning activities of vertebrate hedgehog proteins in the developing eye and brain. Curr Biol. 5, 944-55.

Esteve, P., Bovolenta, P., 2006. Secreted inducers in vertebrate eye development: more functions for old morphogens. Curr Opin Neurobiol. 16, 13-9.

Fitzpatrick, D. R., van Heyningen, V., 2005. Developmental eye disorders. Curr Opin Genet Dev. 15, 348-53.

Flenghi, L., et al., 1995. A specific monoclonal antibody (PG-B6) detects expression of the BCL-6 protein in germinal center B cells. Am J Pathol. 147, 405-11.

Fujita, N., et al., 2004. MTA3 and the Mi-2/NuRD complex regulate cell fate during B lymphocyte differentiation. Cell. 119, 75-86.

Funatsu, N., et al., 2004. Gene expression analysis of the late embryonic mouse cerebral cortex using DNA microarray: identification of several region- and layer-specific genes. Cereb Cortex. 14, 1031-44.

Gearhart, M. D., et al., 2006. Polycomb group and SCF ubiquitin ligases are found in a novel BCOR complex that is recruited to BCL6 targets. Mol Cell Biol. 26, 6880-9.

Goldsmith, P., Harris, W. A., 2003. The zebrafish as a tool for understanding the biology of visual disorders. Semin Cell Dev Biol. 14, 11-8.

Gorlin, R. J., et al., 1996. Oculo-facio-cardio-dental (OFCD) syndrome. Am J Med Genet. 63, 290-2.

Gregory-Evans, C. Y., et al., 2004. Ocular coloboma: a reassessment in the age of molecular neuroscience. J Med Genet. 41, 881-91.

Gross, J. M., Perkins, B. D., 2008. Zebrafish mutants as models for congenital ocular disorders in humans. Mol Reprod Dev. 75, 547-55.

Gross, J. M., et al., 2005. Identification of zebrafish insertional mutants with defects in visual system development and function. Genetics. 170, 245-61.

Hahn, H., et al., 1996. Mutations of the human homolog of Drosophila patched in the nevoid basal cell carcinoma syndrome. Cell. 85, 841-51.

Hallonet, M., et al., 1999. Vax1, a novel homeobox-containing gene, directs development of the basal forebrain and visual system. Genes Dev. 13, 3106-14.

Hallonet, M., et al., 1998. Vax1 is a novel homeobox-containing gene expressed in the developing anterior ventral forebrain. Development. 125, 2599-610.

Hedera, P., Gorski, J. L., 2003. Oculo-facio-cardio-dental syndrome: skewed X chromosome inactivation in mother and daughter suggest X-linked dominant Inheritance. Am J Med Genet A. 123A, 261-6.

Heisenberg, C. P., et al., 1999. Zebrafish aussicht mutant embryos exhibit widespread overexpression of ace (fgf8) and coincident defects in CNS development. Development. 126, 2129-40.

Hero, I., et al., 1991. The prenatal development of the optic fissure in colobomatous microphthalmia. Invest Ophthalmol Vis Sci. 32, 2622-35.

Hiesinger, P. R., et al., 2005. The v-ATPase V0 subunit a1 is required for a late step in synaptic vesicle exocytosis in Drosophila. Cell. 121**,** 607-20.

Hilton, E. N., et al., 2007. Left-sided embryonic expression of the BCL-6 corepressor, BCOR, is required for vertebrate laterality determination. Hum Mol Genet. 16**,** 1773-82.

Hornby, S. J., et al., 2000. Regional variation in blindness in children due to microphthalmos, anophthalmos and coloboma. Ophthalmic Epidemiol. 7**,** 127-38.

Huynh, K. D., et al., 2000. BCoR, a novel corepressor involved in BCL-6 repression. Genes Dev. 14**,** 1810-23.

Jason, L. J., et al., 2005. Histone H2A ubiquitination does not preclude histone H1 binding, but it facilitates its association with the nucleosome. J Biol Chem. 280**,** 4975-82.

Johnson, R. L., et al., 1996. Human homolog of patched, a candidate gene for the basal cell nevus syndrome. Science. 272**,** 1668-71.

Karlstrom, R. O., et al., 1999. Comparative synteny cloning of zebrafish you-too: mutations in the Hedgehog target gli2 affect ventral forebrain patterning. Genes Dev. 13**,** 388-93.

Karlstrom, R. O., et al., 1996. Zebrafish mutations affecting retinotectal axon pathfinding. Development. 123**,** 427-38.

Kawamata, N., et al., 1994. Recognition DNA sequence of a novel putative transcription factor, BCL6. Biochem Biophys Res Commun. 204**,** 366-74.

Kerckaert, J. P., et al., 1993. LAZ3, a novel zinc-finger encoding gene, is disrupted by recurring chromosome 3q27 translocations in human lymphomas. Nat Genet. 5**,** 66-70.

Kim, T. H., et al., 2007. Phactr4 regulates neural tube and optic fissure closure by controlling PP1-, Rb-, and E2F1-regulated cell-cycle progression. Dev Cell. 13**,** 87-102.

Kontani, K., et al., 2005. Repression of cell-cell fusion by components of the C. elegans vacuolar ATPase complex. Dev Cell. 8**,** 787-94.

Koudijs, M. J., et al., 2008. Genetic analysis of the two zebrafish patched homologues identifies novel roles for the hedgehog signaling pathway. BMC Dev Biol. 8**,** 15.

Koudijs, M. J., et al., 2005. The zebrafish mutants dre, uki, and lep encode negative regulators of the hedgehog signaling pathway. PLoS Genet. 1**,** e19.

Leamey, C. A., et al., 2008. Differential gene expression between sensory neocortical areas: potential roles for Ten_m3 and Bcl6 in patterning visual and somatosensory pathways. Cereb Cortex. 18**,** 53-66.

Lee, J., Gross, J. M., 2007. Laminin beta1 and gamma1 containing laminins are essential for basement membrane integrity in the zebrafish eye. Invest Ophthalmol Vis Sci. 48**,** 2483-90.

Lesaffre, B., et al., 2007. Direct non-cell autonomous Pax6 activity regulates eye development in the zebrafish. Neural Dev. 2**,** 2.

Lewis, K. E., et al., 1999. Characterisation of a second patched gene in the zebrafish Danio rerio and the differential response of patched genes to Hedgehog signalling. Dev Biol. 208**,** 14-29.

Liegeois, S., et al., 2006. The V0-ATPase mediates apical secretion of exosomes containing Hedgehog-related proteins in Caenorhabditis elegans. J Cell Biol. 173**,** 949-61.

Locker, M., et al., 2006. Hedgehog signaling and the retina: insights into the mechanisms controlling the proliferative properties of neural precursors. Genes Dev. 20**,** 3036-48.

Logarajah, S., et al., 2003. BCL-6 is expressed in breast cancer and prevents mammary epithelial differentiation. Oncogene. 22**,** 5572-8.

Macdonald, R., et al., 1995. Midline signalling is required for Pax gene regulation and patterning of the eyes. Development. 121**,** 3267-78.

Macdonald, R., et al., 1997. The Pax protein Noi is required for commissural axon pathway formation in the rostral forebrain. Development. 124**,** 2397-408.

Manners, R. M., et al., 1996. Microphthalmos in association with Gorlin's syndrome. Br J Ophthalmol. 80**,** 378.

Migliazza, A., et al., 1995. Frequent somatic hypermutation of the 5' noncoding region of the BCL6 gene in B-cell lymphoma. Proc Natl Acad Sci U S A. 92**,** 12520-4.

Ming, J. E., et al., 2002. Mutations in PATCHED-1, the receptor for SONIC HEDGEHOG, are associated with holoprosencephaly. Hum Genet. 110**,** 297-301.

Mui, S. H., et al., 2002. The homeodomain protein Vax2 patterns the dorsoventral and nasotemporal axes of the eye. Development. 129**,** 797-804.

Mui, S. H., et al., 2005. Vax genes ventralize the embryonic eye. Genes Dev. 19**,** 1249-59.

Nakayama, Y., et al., 2008. Fgf19 is required for zebrafish lens and retina development. Dev Biol. 313**,** 752-66.

Nelson, N., Harvey, W. R., 1999. Vacuolar and plasma membrane proton-adenosinetriphosphatases. Physiol Rev. 79**,** 361-85.

Neuhauss, S. C., et al., 1999. Genetic disorders of vision revealed by a behavioral screen of 400 essential loci in zebrafish. J Neurosci. 19**,** 8603-15.

Ng, D., et al., 2004. Oculofaciocardiodental and Lenz microphthalmia syndromes result from distinct classes of mutations in BCOR. Nat Genet. 36**,** 411-6.

Nieuwkoop, P. D., Faber, J., 1994. Normal Table of *Xenopus laevis* (Daudin). Garland, New York.

Nishi, T., Forgac, M., 2002. The vacuolar (H+)-ATPases--nature's most versatile proton pumps. Nat Rev Mol Cell Biol. 3**,** 94-103.

Niu, H., et al., 1998. Antigen receptor signaling induces MAP kinase-mediated phosphorylation and degradation of the BCL-6 transcription factor. Genes Dev. 12**,** 1953-61.

Nuckels, R. J., et al., 2009. The vacuolar-ATPase complex regulates retinoblast proliferation and survival, photoreceptor morphogenesis, and pigmentation in the zebrafish eye. Invest Ophthalmol Vis Sci. 50**,** 893-905.

Ohno, H., 2004. Pathogenetic role of BCL6 translocation in B-cell non-Hodgkin's lymphoma. Histol Histopathol. 19, 637-50.

Ohsaki, K., et al., 1999. Expression of the Vax family homeobox genes suggests multiple roles in eye development. Genes Cells. 4, 267-76.

Onizuka, T., et al., 1995. BCL-6 gene product, a 92- to 98-kD nuclear phosphoprotein, is highly expressed in germinal center B cells and their neoplastic counterparts. Blood. 86, 28-37.

Otaki, J. M., et al., 2005. The proto-oncogene BCL-6 is expressed in olfactory sensory neurons. Neurosci Res. 53, 189-200.

Otaki, J. M., et al., The proto-oncogene BCL6 promotes survival of olfactory sensory neurons. Dev Neurobiol. 70, 424-35.

Otteson, D. C., et al., 1998. Pax2 expression and retinal morphogenesis in the normal and Krd mouse. Dev Biol. 193, 209-24.

Pasqualucci, L., et al., 2003. Mutations of the BCL6 proto-oncogene disrupt its negative autoregulation in diffuse large B-cell lymphoma. Blood. 101, 2914-23.

Perron, M., et al., 2003. A novel function for Hedgehog signalling in retinal pigment epithelium differentiation. Development. 130, 1565-77.

Phan, R. T., Dalla-Favera, R., 2004. The BCL6 proto-oncogene suppresses p53 expression in germinal-centre B cells. Nature. 432, 635-9.

Polo, J. M., et al., 2004. Specific peptide interference reveals BCL6 transcriptional and oncogenic mechanisms in B-cell lymphoma cells. Nat Med. 10, 1329-35.

Porges, Y., 1995. Autosomal dominant typical coloboma associated with unilateral pseudoptosis, myopia and cataract. Cent Afr J Med. 41, 255-7.

Rao, B., et al., 2005. Dimethylation of histone H3 at lysine 36 demarcates regulatory and nonregulatory chromatin genome-wide. Mol Cell Biol. 25, 9447-59.

Roessler, E., et al., 1996. Mutations in the human Sonic Hedgehog gene cause holoprosencephaly. Nat Genet. 14, 357-60.

Sakano, D., et al., BCL6 canalizes Notch-dependent transcription, excluding Mastermind-like1 from selected target genes during left-right patterning. Dev Cell. 18, 450-62.

Sanyanusin, P., et al., 1995. Mutation of the PAX2 gene in a family with optic nerve colobomas, renal anomalies and vesicoureteral reflux. Nat Genet. 9, 358-64.

Sasagawa, S., et al., 2002. Axes establishment during eye morphogenesis in Xenopus by coordinate and antagonistic actions of BMP4, Shh, and RA. Genesis. 33, 86-96.

Schauerte, H. E., et al., 1998. Sonic hedgehog is not required for the induction of medial floor plate cells in the zebrafish. Development. 125, 2983-93.

Schulze, B. R., et al., 1999. Rare dental abnormalities seen in oculo-facio-cardio-dental (OFCD) syndrome: three new cases and review of nine patients. Am J Med Genet. 82, 429-35.

Schwarz, M., et al., 2000. Spatial specification of mammalian eye territories by reciprocal transcriptional repression of Pax2 and Pax6. Development. 127, 4325-34.

Seyfert, V. L., et al., 1996. Transcriptional repression by the proto-oncogene BCL-6. Oncogene. 12, 2331-42.

Stadler, J. A., et al., 2005. Histone deacetylase 1 is required for cell cycle exit and differentiation in the zebrafish retina. Dev Dyn. 233**,** 883-9.

Sterner, D. E., Berger, S. L., 2000. Acetylation of histones and transcription-related factors. Microbiol Mol Biol Rev. 64**,** 435-59.

Stogios, P. J., et al., 2005. Sequence and structural analysis of BTB domain proteins. Genome Biol. 6**,** R82.

Taipale, J., et al., 2002. Patched acts catalytically to suppress the activity of Smoothened. Nature. 418**,** 892-7.

Take-uchi, M., et al., 2003. Hedgehog signalling maintains the optic stalk-retinal interface through the regulation of Vax gene activity. Development. 130**,** 955-68.

Torres, M., et al., 1996. Pax2 contributes to inner ear patterning and optic nerve trajectory. Development. 122**,** 3381-91.

Tsukada, Y., et al., 2006. Histone demethylation by a family of JmjC domain-containing proteins. Nature. 439**,** 811-6.

Wallace, D. M., Cotter, T. G., 2009. Histone deacetylase activity in conjunction with E2F-1 and p53 regulates Apaf-1 expression in 661W cells and the retina. J Neurosci Res. 87**,** 887-905.

Wallace, D. M., et al., 2006. Histone deacetylase activity regulates apaf-1 and caspase 3 expression in the developing mouse retina. Invest Ophthalmol Vis Sci. 47**,** 2765-72.

Wang, H., et al., 2004. Role of histone H2A ubiquitination in Polycomb silencing. Nature. 431**,** 873-8.

Wolff, C., et al., 2003. Multiple muscle cell identities induced by distinct levels and timing of hedgehog activity in the zebrafish embryo. Curr Biol. 13**,** 1169-81.

Wong, C. W., Privalsky, M. L., 1998. Components of the SMRT corepressor complex exhibit distinctive interactions with the POZ domain oncoproteins PLZF, PLZF-RARalpha, and BCL-6. J Biol Chem. 273**,** 27695-702.

Yamaguchi, M., et al., 2005. Histone deacetylase 1 regulates retinal neurogenesis in zebrafish by suppressing Wnt and Notch signaling pathways. Development. 132**,** 3027-43.

Yamamoto, Y., et al., 2004. Hedgehog signalling controls eye degeneration in blind cavefish. Nature. 431**,** 844-7.

Ye, B. H., et al., 1995. Chromosomal translocations cause deregulated BCL6 expression by promoter substitution in B cell lymphoma. EMBO J. 14**,** 6209-17.

Ye, B. H., et al., 1993. Cloning of bcl-6, the locus involved in chromosome translocations affecting band 3q27 in B-cell lymphoma. Cancer Res. 53**,** 2732-5.

Zhang, X. M., Yang, X. J., 2001. Temporal and spatial effects of Sonic hedgehog signaling in chick eye morphogenesis. Dev Biol. 233**,** 271-90.

Zollman, S., et al., 1994. The BTB domain, found primarily in zinc finger proteins, defines an evolutionarily conserved family that includes several developmentally regulated genes in Drosophila. Proc Natl Acad Sci U S A. 91**,** 10717-21.

Vita

Jiwoon Lee was born in Seoul, Korea on July 17, 1978, the son of Dae-Hee Lee and Kum-Soon Lee. After graduating from Bosung High School, Seoul, Korea, in 1997, he entered to Korea Advanced Institute of Science and Technology. He received a Bachelor of Science degree in Biological Science in 2001 and a Master of Science degree in 2004. In August 2005, he entered The University of Texas in the Institute for Cellular and Molecular Biology graduate program.

Permanent address: 9417 Great Hills Trail #2095

Austin, TX 78759

E-mail address: talk2jiwoon@hotmail.com

This dissertation was typed by the author.